

Frequency Response Identification of Low-Order Systems: Finite-Sample Analysis

Arya Honarpisheh, Mario Sznaier

Abstract—This paper proposes a frequency-domain system identification method for learning low-order systems. The identification problem is formulated as the minimization of the ℓ_2 norm between the identified and measured frequency responses, with the nuclear norm of the Loewner matrix serving as a regularization term. This formulation results in an optimization problem that can be efficiently solved using standard convex optimization techniques. We derive an upper bound on the sampled-frequency complexity of the identification process and subsequently extend this bound to characterize the identification error over all frequencies. A detailed analysis of the sample complexity is provided, along with a thorough interpretation of its terms and dependencies. Finally, the efficacy of the proposed method is demonstrated through an example, and numerical simulations validating the growth rate of the sample complexity bound.^{1 2}

Index Terms—finite-time identification, frequency-domain identification, linear systems, low-order systems, machine learning, sample complexity, statistical learning, system identification

I. INTRODUCTION

System identification is the process of constructing a mathematical model of a dynamical system from observed data, which may be collected in either the time or frequency domain [1]. Traditionally, most theoretical developments in system identification have been established under asymptotic assumptions, where the number of samples tends to infinity [2]. In recent years, however, there has been growing interest in non-asymptotic approaches that provide guarantees with finite data [3]–[8]. The present work follows this direction.

In parallel, the control of dynamical systems has increasingly incorporated ideas from machine learning, seeking to enhance both identification and control capabilities. Notable examples include data-driven control strategies [9]–[11], neural-network-based controllers [12]–[14], learning-based sparse sensing [15], and reinforcement learning for control [16]. This broader integration of learning-based methods into the identification and control motivates our study of system

identification in finite-sample regimes. Leveraging tools from learning theory [17]–[19], we investigate the non-asymptotic identification of low-order linear time-invariant (LTI) systems in the frequency domain.

Frequency-domain identification focuses on modeling systems based on their responses at different frequencies [20]. Several methods have been proposed in the literature, ranging from classical techniques such as maximum likelihood, least squares [21], and interpolation-based methods [22] to more recent approaches, such as Gaussian processes [23] and non-convex optimization [24].

Low-order models offer simplified representations of dynamical systems, which can significantly enhance computational efficiency and interpretability in system analysis, controller design, and real-time signal processing. One notable approach to low-order system identification involves minimizing the rank of the Hankel matrix constructed from the system’s impulse response [25]. An alternative method, based on adopting a suitable regularizer [26], has been proposed in [27]. A different method, which selects a small number of poles (called atoms), was proposed in [28]. Additionally, a frequency-domain approach that transforms data from frequency to time domain, thereby facilitating the formation of a Hankel matrix, has been presented in [29]. A fast and easy-to-implement algorithm for mixed time-frequency data, based on nuclear norm minimization of the Hankel matrix with interpolation constraints, was proposed in [30].

The sample complexity of an identification algorithm is of paramount importance, as it provides valuable insights into the amount of data required to identify a system with a desired level of accuracy [31]. The resulting bounds measure the gap between the identified and the true model and thereby calibrate robustness margins in controller synthesis; Sharper bounds provide less conservative designs in robust control approaches such as [32]. Although numerous results on the sample complexity of LTI systems exist [33]–[40], fewer studies specifically address low-order methods. In the time domain, several works have established sample complexity bounds for low-order identification of LTI systems such as [41], [42]. In contrast, in the frequency domain, sample complexity bounds remain largely unexplored. The recent work by [43] investigates the sample complexity for the classical empirical transfer function estimation approach [44]. We fill a gap in the literature concerning the sample complexity of identifying low-order systems in the frequency domain by proposing a method based on the nuclear norm minimization of the Loewner matrix constructed from the frequency response.

This work was partially supported by NSF grants CNS–2038493 and CMMI–2208182, AFOSR grant FA9550-19-1-0005 and ONR grant N00014-21-1-2431.

Arya Honarpisheh and Mario Sznaier are with the Robust Systems Lab, ECE Department, Northeastern University, Boston, MA 02115 USA (e-mail: honarpisheh.a@northeastern.edu, msznaier@coe.neu.edu).

¹Code available at https://github.com/Arya-Honarpisheh/freq_iden_low_order.

²This work has been submitted to the IEEE for possible publication. Copyright may be transferred without notice, after which this version may no longer be accessible.

Loewner matrices play a critical role in interpolation-based system identification and model order reduction in both the time and frequency domains [45]. Additionally, the Loewner framework has been extended to certain subclasses of nonlinear systems [46], implemented on networked systems [47], and combined with other system identification methods as a model order reduction technique [48]. Several studies have addressed the identification of low-order systems within the Loewner framework. [49] proposed a convex optimization-based method that enforces consistency with the gathered data and guarantees stability through optimization constraints, which was later extended to a two-step identification approach using linear fractional transformations [50].

In this paper, we address the problem of learning a low-order LTI system from frequency-domain data. Our proposed method is distinct from those above in that it incorporates the nuclear norm of the Loewner matrix as a regularizer rather than as a constraint, analogous to the Hankel nuclear norm regularization [25] in the time domain. The key contributions of this work are summarized as follows:

- We propose a computationally efficient method to identify an LTI system when data are provided in the frequency domain. Our approach leverages the inherent properties of the Loewner matrix to promote low-order system representations.
- We provide an extensive theoretical analysis of the proposed method by deriving upper bounds on its sample complexity over a fixed set of frequencies, which is subsequently extended to cover the entire frequency range. In particular, we show that the sample complexity grows at the rate of $\mathcal{O}\left(\sqrt{\frac{M \ln M}{N}}\right)$, where M denotes the number of frequency points and N represents the number of measured responses at each frequency.
- We demonstrate the effectiveness of the proposed approach in identifying low-order systems through numerical simulations.
- We run Monte Carlo simulations to numerically validate the growth rate of the theoretical sample complexity bound with respect to the parameters.

This paper is organized as follows. Section II introduces the notation. Section II-B rigorously formulates the identification problem and presents the identification method. Section III states the assumptions for our analysis, develops key properties of the Loewner operator, and derives the sample-complexity bound. Section IV reports numerical experiments on learning low-order systems and validates the bound. Section V concludes the paper. For the sake of readability, some necessary technical results and proofs are presented in the Appendices.

II. PRELIMINARIES

A. Notation

For a vector \mathbf{x} , its r^{th} element is denoted by x_r . For a matrix \mathbf{X} , the element in the r th row and s th column is represented by x_{rs} , while the s th column is denoted by \mathbf{x}_s .

Given a matrix \mathbf{X} , its conjugate transpose is denoted by \mathbf{X}^* . The inner product on the space of matrices is defined as

$\mathbb{Z}(\mathbb{Z}^+)$	Set of integers (nonnegative integers)
$\mathbb{R}^n(\mathbb{C}^n)$	Set of real (complex) n -tuples
\mathbb{D}	Unit disk in the complex plane
\mathbb{D}_ρ	Disk with radius ρ in the complex plane
$\mathbb{R}^{n \times m}(\mathbb{C}^{n \times m})$	Set of $n \times m$ real (complex) matrices
$ z (\arg(z))$	Absolute value (argument) of the complex number z
\bar{z}	Conjugate of the complex number z
$\Re(z)(\Im(z))$	Real(Imaginary) part of the complex number z
$\mathbf{0}_n(\mathbf{1}_n)$	The n -dimensional vector of all zeros(ones)
\mathbf{e}_k	The k -th vector of the standard basis of \mathbb{R}^n
\mathbf{I}_n	The $n \times n$ identity matrix
$\mathbf{0}_{n \times m}$	The $n \times m$ matrix of all zeros
$\ \mathbf{x}\ _p$	ℓ_p -norm of vector \mathbf{x}
$\ \mathbf{X}\ _p$	p -operator norm of matrix \mathbf{X}
$\ \mathbf{X}\ _*$	Nuclear norm of matrix \mathbf{X}
$\ \mathbf{X}\ _F$	Frobenius norm of matrix \mathbf{X}
$\text{Tr}(\mathbf{X})$	Trace of matrix \mathbf{X}

$\langle \mathbf{X}, \mathbf{Y} \rangle = \text{Tr}(\mathbf{X}^* \mathbf{Y})$. \mathbf{X}^\dagger indicates the pseudo-inverse of the matrix \mathbf{X} .

Let $L : \mathcal{H} \rightarrow \mathcal{K}$ be a linear operator between Hilbert spaces \mathcal{H} and \mathcal{K} . The adjoint operator of L is denoted by L^* .

For a real-valued function $f : \mathcal{H} \rightarrow \mathbb{R}$ defined on the Hilbert space \mathcal{H} , the subdifferential of f is denoted by ∂f .

Let \mathcal{S} denote the set of discrete-time, causal, finite-dimensional LTI systems. Each system is characterized by its impulse response, denoted by the function $g : \mathbb{Z}^+ \rightarrow \mathbb{R}$. The corresponding transfer function is represented by $G : \mathbb{C} \rightarrow \mathbb{C}$ and is defined as $G(z) = \sum_{k=0}^{\infty} g(k)z^k$ ³. A realization of a system in \mathcal{S} is a state-space model:

$$\begin{aligned} \mathbf{x}(k+1) &= \mathbf{A}\mathbf{x}(k) + \mathbf{B}\mathbf{u}(k) \\ \mathbf{y}(k) &= \mathbf{C}\mathbf{x}(k) + \mathbf{D}\mathbf{u}(k), \end{aligned}$$

with the state variable $\mathbf{x} \in \mathbb{R}^n$, such that

$$G(z) = \mathbf{C}(z^{-1}\mathbf{I}_n - \mathbf{A})^{-1}\mathbf{B} + \mathbf{D}. \quad (1)$$

The subset of \mathcal{S} consisting of systems whose transfer function is analytic on \mathbb{D}_ρ and whose absolute value is bounded by K is denoted by $\mathcal{H}_\infty(\rho, K)$. We define the \mathcal{H}_∞ norm of a system that is analytic on \mathbb{D} as

$$\|G\|_\infty = \sup_{z \in \mathbb{D}} |G(z)|,$$

and its \mathcal{H}_2 norm as

$$\|G\|_2 = \sqrt{\frac{1}{2\pi} \int_{-\pi}^{\pi} |G(e^{j\theta})|^2 d\theta} = \sqrt{\sum_{k=0}^{\infty} g(k)^2} = \|g\|_2,$$

where the equality comes from Parseval's Theorem.

B. Problem Statement

We address the problem of learning a system in the frequency domain. The experimental data $D = (z, \tilde{\mathbf{W}})$ consists of N samples at M different frequencies:

$$\mathbf{z} = \begin{bmatrix} z_1 \\ \vdots \\ z_M \end{bmatrix} \quad \tilde{\mathbf{W}} = \begin{bmatrix} \tilde{w}_{1,1} & \cdots & \tilde{w}_{1,N} \\ \vdots & \ddots & \vdots \\ \tilde{w}_{M,1} & \cdots & \tilde{w}_{M,N} \end{bmatrix} \quad (2)$$

³The transfer function defined herein differs from the standard notation in the literature, where the conventional transfer function is expressed as $G\left(\frac{1}{z}\right)$. For stable systems, the function $G(z)$ is analytic inside the unit disk.

$$\mathbf{V} = \begin{bmatrix} v_{1,1} & \cdots & v_{1,N} \\ \vdots & \ddots & \vdots \\ v_{M,1} & \cdots & v_{M,N} \end{bmatrix} \quad \tilde{\mathbf{W}} = \bar{\mathbf{W}} + \mathbf{V} \quad (3)$$

where \mathbf{z} represents the frequency points on the upper unit semicircle. The true and measured frequency responses of the system at these points are denoted by $\bar{\mathbf{W}}$ and $\tilde{\mathbf{W}}$, respectively. The process noise is represented by \mathbf{V} . The goal is to develop a learning algorithm that identifies a low-order system \hat{G} capable of generating the experimental data D from the true system \bar{G} . Moreover, we are interested in the nonasymptotic properties of the identification algorithm: For any $\epsilon > 0$ and $\delta > 0$, there exists a finite number $N_{\text{sc}}(\epsilon, \delta)$ such that, for $N \geq N_{\text{sc}}$,

$$\text{Prob} \left(\|\hat{G} - \bar{G}\|_{\infty} \leq \epsilon \right) \geq 1 - \delta. \quad (4)$$

The number N_{sc} is referred to as the *sample complexity* of the identification algorithm.

In this paper, we propose to recast the problem above into a regularized *Loewner Nuclear Norm Minimization (LNNM)* of the form:

$$\hat{\mathbf{w}} = \underset{\mathbf{w} \in \mathbb{C}^M}{\text{argmin}} \tau \frac{\|L(\mathbf{w})\|_*}{M} + \frac{1}{2} \sum_{s=1}^N \|\mathbf{w} - \tilde{\mathbf{w}}_s\|_2^2, \quad (5)$$

where $\tau > 0$ is a regularization parameter. Here $\hat{\mathbf{w}}$ denotes the frequency response of the identified system at the frequency points \mathbf{z} and $L(\mathbf{w})$ is the Loewner matrix obtained by partitioning the data into two subsets, $\mathbf{z}^{(a)}, \mathbf{w}^{(a)} \in \mathbb{C}^p$ and $\mathbf{z}^{(b)}, \mathbf{w}^{(b)} \in \mathbb{C}^q$, and defining

$$L(\mathbf{w}) \doteq \begin{bmatrix} \frac{w_1^{(b)} - w_1^{(a)}}{z_1^{(b)} - z_1^{(a)}} & \cdots & \frac{w_p^{(b)} - w_p^{(a)}}{z_1^{(b)} - z_p^{(a)}} \\ \vdots & \ddots & \vdots \\ \frac{w_q^{(b)} - w_1^{(a)}}{z_q^{(b)} - z_1^{(a)}} & \cdots & \frac{w_q^{(b)} - w_p^{(a)}}{z_q^{(b)} - z_p^{(a)}} \end{bmatrix}. \quad (6)$$

The Loewner matrix plays a central role in the interpolation of rational matrix functions [51]. Specifically, if the data points $(\mathbf{z}^{(a)}, \mathbf{w}^{(a)})$ and $(\mathbf{z}^{(b)}, \mathbf{w}^{(b)})$ are such that the underlying transfer function $G(z)$ satisfies $G(z_k^{(a)}) = w_k^{(a)}$ and $G(z_k^{(b)}) = w_k^{(b)}$, then a state-space realization of G can be derived from $L(\mathbf{w})$ using Theorem 4.1 in [51].

Remark 1: The objective in (5) balances fidelity to the data against the order of the identified system. Selecting the lowest-order system that explains the observed data is, in general, a challenging task. It is well-known that the system's order is equivalent to the rank of the Loewner matrix [51]. However, rank minimization problems are generally NP-hard. To address this, we use the nuclear norm of the Loewner matrix as a convex surrogate for the rank function [52], which promotes low-rank solutions while preserving computational tractability.

Remark 2: Our formulation addresses system identification when frequency-domain measurements are available. This perspective is particularly appealing because frequency-domain data may capture system dynamics more effectively, especially when a low-order system is desirable for operation within a limited frequency band [53] or when the system operates near the stability threshold, where an extensive amount of

time-domain data would be required [54]. Another aspect addressed here is the emphasis on low-order representations, which results in reduced computational resources for filtering and control, as well as enhanced performance when model order reduction is subsequently applied [55]. Moreover, our focus on sample complexity aligns with the growing interest in non-asymptotic analysis of identification algorithms [56], thereby addressing the challenges associated with deriving finite-sample bounds in system identification.

Remark 3: Compared to other convex optimization-based methods for identifying low-order systems in frequency domain [49], [50], the proposed approach does not impose stability and consistency conditions as explicit constraints. Instead, the identification problem is reformulated as an unconstrained optimization by minimizing the sum-of-squares error while incorporating the nuclear norm of the Loewner matrix as a regularizer. This strategy is analogous to the Hankel nuclear norm regularization approach in the time domain proposed in [25]. Furthermore, the nuclear norm of the Loewner matrix is scaled by the number of frequency points, since $\frac{\|L(\mathbf{w})\|_*}{M}$ converges to the trace norm of the system i.e. the sum of the singular values of the Hankel operator (Theorem 1 in [50]). Consequently, as an unconstrained convex optimization problem, the proposed method is computationally efficient, and its efficiency can even be further improved using proximal gradient methods or the multiplier alternating direction method [57], given that the cost function can be split into the sum of two closed, proper, convex functions. Although the method is presented for the single-input-single-output (SISO) systems, it is anticipated that extending the approach to multi-input-multi-output (MIMO) systems would be straightforward, as the desirable properties of the Loewner matrix naturally extend to such systems. For the sake of the non-asymptotic analysis, however, the focus here is restricted to the SISO systems.

III. SAMPLE COMPLEXITY ANALYSIS

In this section we present the main result of the paper: a sample complexity analysis showing that, with high probability, the solution of (5) satisfies $\|\hat{\mathbf{w}} - \bar{\mathbf{w}}\|_{\infty} \leq \mathcal{O}(N^{-1/2})$, which aligns with the general expectations for identification errors. To establish these results, we will proceed along the following road map

- 1: Define a *linear* Loewner operator $L(\cdot)$ and characterize its adjoint $L^*(\cdot)$.
- 2: Bound the identification error in terms of the minimum gain of $L(\cdot)$ and the maximum norm of $L^{-*}((v))$, that is, the image of the noise under the inverse of $L^*(\cdot)$.
- 3: Bound the minimum gain of $L(\cdot)$ over a suitably defined cone.
- 3: Use a concentration of measure inequality to bound $L^{-*}((v))$ with high probability.
- 4: Combine these in a bound that depends only on the problem data.

We make the following assumptions throughout the rest of the paper:

Assumption 1: The true system \bar{G} belongs to $\mathcal{H}_{\infty}(\rho, K)$, where $\rho > 1$ and $K > 0$. In other words, its impulse response

decays exponentially with the rate of the inverse of ρ , i.e., $|g(t+k)| \leq K|g(t)|\rho^{-k}$ for all $t, k \in \mathbb{Z}^+$.

Assumption 2: The noise has zero mean, i.e., $\mathbb{E}(v_{r,s}) = 0$, is independent across experiments and frequencies (It does not need to be identically distributed), and is almost surely bounded such that $\mathbb{P}(|v_{r,s}| \leq \eta_r) = 1$, where the bound η_r depends on the frequency. Consequently, $v_{r,s}$ is a sub-Gaussian random variable with variance η_r^2 . We denote by $\bar{\eta} = \max_{r \leq M}(\eta_r)$ the worst-case noise bound across all frequencies.

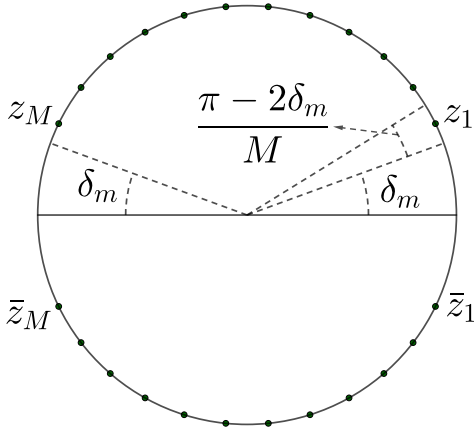


Fig. 1. *Frequency Points z* : Equally spaced points on the upper half of the unit circle with margin δ_m from 0 and π .

Assumption 3: The frequency points z_r are equally spaced on the upper half of the unit circle, i.e., $z_r = e^{j\theta_r}$, where $\theta_r = \delta_m + \frac{\pi - 2\delta_m}{M}(r - \frac{1}{2})$ for $r = 1, \dots, M$. The parameter $0 < \delta_m < \pi$ is referred to as the frequency margin. Refer to figure 1 for a visualization of z .

Remark 4: Although our proposed method can be readily applied to the identification of LTI systems without these technical assumptions, they are essential for the derivation of the sample complexity bounds.

- Assumption 1 is a standard stability assumption; the analysis in this paper relies on the exponential decay of the impulse response for strictly stable systems ($\rho > 1$).
- Assumption 2 is a standard bounded noise assumption. We believe that this assumption is not overly restrictive, as the analysis can be modified to accommodate alternative noise distributions (e.g., Gaussian or colored noise) by leveraging concentration inequalities different from Theorem 3.
- Assumption 3 is a new assumption introduced in this paper; it requires that there exists a margin from 0 and π for the frequency points z . Although δ_m appears in the sample complexity bound, for any finite number of z , as long as 1 and -1 are not included in z , such a positive δ_m can be found. Conversely, if 1 or -1 are present in z , they may be disregarded. Technically, the frequency response at 1 corresponds to the DC gain of the system. In practice, it is not used to construct the Loewner matrix but is instead employed later to determine the input-to-output matrix D , as discussed in Remark 5. The requirement that these points be equally spaced is necessary in the

proof to approximate an integral using the midpoint rule. This condition can be relaxed if an alternative result on numerical integration error, which accounts for non-equally spaced points, is used.

A. The Loewner Operator and its Adjoint

1) *Loewner Operator:* Given fixed frequencies z , define the complex Loewner operator $L_c(\mathbf{w}) : \mathbb{C}^M \rightarrow \mathbb{C}^{M \times M}$ as

$$L_c(\mathbf{w}) = \begin{bmatrix} \frac{\bar{w}_1 - w_1}{z_1 - z_1} & \frac{\bar{w}_1 - w_2}{z_1 - z_2} & \dots & \frac{\bar{w}_1 - w_M}{z_1 - z_M} \\ \frac{\bar{w}_2 - w_1}{z_2 - z_1} & \frac{\bar{w}_2 - w_2}{z_2 - z_2} & \dots & \frac{\bar{w}_2 - w_M}{z_2 - z_M} \\ \vdots & \vdots & \ddots & \vdots \\ \frac{\bar{w}_M - w_1}{z_M - z_1} & \frac{\bar{w}_M - w_2}{z_M - z_2} & \dots & \frac{\bar{w}_M - w_M}{z_M - z_M} \end{bmatrix}. \quad (7)$$

The Loewner operator returns the Loewner matrix, as defined in (6), where $z^{(a)}$ are taken to be z and $w^{(b)}$ are their conjugates \bar{z} . It is important to note that this operator is not linear over the field of complex numbers, as complex conjugation is inherently non-linear. However, when interpreted as a function defined over \mathbb{R}^{2M} , the operator exhibits linearity. To formalize this perspective, we define the real Loewner operator $L_r : \mathbb{R}^{2M} \rightarrow \mathbb{C}^{M \times M}$ as follows:

$$L_r \left(\begin{bmatrix} \mathbf{a} \\ \mathbf{b} \end{bmatrix} \right) = L_c(\mathbf{a} + j\mathbf{b}). \quad (8)$$

Let $\mathbf{w} \in \ker(L_r)$, then all the entries of $L_r(\mathbf{w})$ are zero. From the requirement that all diagonal entries vanish, it follows that w_k is real for each k . The condition that all off-diagonal entries are also zero further implies that $w_1 = \dots = w_M$. Consequently, the real Loewner operator is not invertible, and its nontrivial kernel is given by $\ker(L_r) = \begin{bmatrix} \mathbf{1}_M \\ \mathbf{0}_M \end{bmatrix}$.

Denote the space of all Loewner matrices as $\mathbb{L}(M) = L_c(\mathbb{C}^M) = L_r(\mathbb{R}^{2M})$, and define the invertible version of L_r as the Loewner operator $L : \mathbb{R}^{2M} \rightarrow \mathbb{L}(M)$. For any $\mathbf{X} \in \mathbb{L}(M)$, the inverse of \mathbf{X} under L is defined as the unique element in $L_r^{-1}(\mathbf{X})$ that has the minimum Euclidean norm. Thus, $L^{-1}(\mathbf{X})$ is given by $\begin{bmatrix} \Re \mathbf{w} \\ \Im \mathbf{w} \end{bmatrix}$ such that $\sum \Re \mathbf{w} = 0$ since if $\begin{bmatrix} \Re \mathbf{w} \\ \Im \mathbf{w} \end{bmatrix} \in L_r^{-1}(\mathbf{X})$, then for any $\lambda \in \mathbb{R}$, $\begin{bmatrix} \Re \mathbf{w} \\ \Im \mathbf{w} \end{bmatrix} + \lambda \begin{bmatrix} \mathbf{1}_M \\ \mathbf{0}_M \end{bmatrix}$ also belongs to $L_r^{-1}(\mathbf{X})$.

Remark 5: The reason that the real Loewner operator is not invertible is that, from the Loewner matrix (6), one can add a real number to all w and still obtain the same Loewner matrix. For this reason, in practice, there exists a degree of freedom in constructing a realization from $L_c(\mathbf{w})$. For example, Theorem 4.1 in [51] provides a realization constructed from the Loewner matrix in which the input-to-output matrix D is a free variable. This corresponds to adding a real number to the transfer function, as demonstrated in (1).

2) *Adjoint of the Loewner Operator and its Inverse:* To compute the adjoint operator of L , define the Loewner matrices \mathbf{E}_k and \mathbf{F}_k for $k = 1, \dots, M$ as

$$(\mathbf{E}_k)_{rs} = \begin{cases} \frac{1}{z_k - z_s} & r = k \text{ and } s \neq k \\ \frac{-1}{z_r - z_k} & r \neq k \text{ and } s = k \\ 0 & r = s = k \\ 0 & \text{otherwise} \end{cases} \quad (9)$$

and

$$(\mathbf{F}_k)_{rs} = \begin{cases} \frac{-j}{\bar{z}_k - z_s} & r = k \text{ and } s \neq k \\ \frac{-j}{\bar{z}_r - z_k} & r \neq k \text{ and } s = k \\ \frac{-2j}{\bar{z}_k - z_k} & r = s = k \\ 0 & \text{otherwise.} \end{cases} \quad (10)$$

Clearly, $L\left(\begin{bmatrix} \mathbf{e}_k \\ \mathbf{0}_M \end{bmatrix}\right) = \mathbf{E}_k$ and $L\left(\begin{bmatrix} \mathbf{0}_M \\ \mathbf{e}_k \end{bmatrix}\right) = \mathbf{F}_k$, and thus, $\{\mathbf{E}_k, \mathbf{F}_k\}_{k=1}^M$ form a basis for the space of all Loewner matrices. Therefore, the *adjoint Loewner operator* $L^* : \mathbb{L}(M) \rightarrow \mathbb{C}^M$ is

$$L^*(\mathbf{X}) = \begin{bmatrix} \langle \mathbf{E}_1, \mathbf{X} \rangle \\ \vdots \\ \langle \mathbf{E}_M, \mathbf{X} \rangle \\ \langle \mathbf{F}_1, \mathbf{X} \rangle \\ \vdots \\ \langle \mathbf{F}_M, \mathbf{X} \rangle \end{bmatrix} \quad (11)$$

for all $\mathbf{X} \in \mathbb{L}(\mathbf{X})$.

To find the inverse of the adjoint of the Loewner operator, we follow the definition of the inverse operator; $\mathbf{X} = L^{-*}\left(\begin{bmatrix} \mathbf{a} \\ \mathbf{b} \end{bmatrix}\right)$ iff $L^*(\mathbf{X}) = \begin{bmatrix} \mathbf{a} \\ \mathbf{b} \end{bmatrix}$. Thus,

$$L^{-*}\left(\begin{bmatrix} \mathbf{a} \\ \mathbf{b} \end{bmatrix}\right) = \mathbf{X} \text{ iff } a_k = \langle \mathbf{E}_k, \mathbf{X} \rangle \text{ and } b_k = \langle \mathbf{F}_k, \mathbf{X} \rangle. \quad (12)$$

Because $\{\mathbf{E}_k, \mathbf{F}_k\}_{k=1}^M$ is a basis for $\mathbb{L}(M)$, there exists unique $\mathbf{c}, \mathbf{d} \in \mathbb{R}^M$ such that $\mathbf{X} = \sum_{k=1}^M c_k \mathbf{E}_k + \sum_{k=1}^M d_k \mathbf{F}_k$. Thus, taking the inner products $\langle \mathbf{E}_r, \mathbf{X} \rangle$ and $\langle \mathbf{F}_r, \mathbf{X} \rangle$ results in the following system of linear equations:

$$\begin{bmatrix} \langle \mathbf{E}_r, \mathbf{E}_k \rangle & \langle \mathbf{E}_r, \mathbf{F}_k \rangle \\ \langle \mathbf{F}_r, \mathbf{E}_k \rangle & \langle \mathbf{F}_r, \mathbf{F}_k \rangle \end{bmatrix} \begin{bmatrix} \mathbf{c} \\ \mathbf{d} \end{bmatrix} = \begin{bmatrix} \mathbf{a} \\ \mathbf{b} \end{bmatrix}. \quad (13)$$

Due to the structure of \mathbf{E}_k and \mathbf{F}_k described in (9) and (10), the off-diagonal block matrices in the LHS of (13) are zero. Thus, the *inverse adjoint Loewner operator* is

$$L^{-*}\left(\begin{bmatrix} \mathbf{a} \\ \mathbf{b} \end{bmatrix}\right) = \sum_{k=1}^M \left(\mathbf{e}_k^\top \mathbf{E}_{\text{in}}^\dagger \mathbf{a} \mathbf{E}_k \right) + \sum_{k=1}^M \left(\mathbf{e}_k^\top \mathbf{F}_{\text{in}}^{-1} \mathbf{b} \mathbf{F}_k \right). \quad (14)$$

in which $\mathbf{E}_{\text{in}}, \mathbf{F}_{\text{in}} \in \mathbb{C}^{M \times M}$ are such that $(\mathbf{E}_{\text{in}})_{rk} = \langle \mathbf{E}_r, \mathbf{E}_k \rangle$ and $(\mathbf{F}_{\text{in}})_{rk} = \langle \mathbf{F}_r, \mathbf{F}_k \rangle$. Similar to the Loewner matrix, the matrix \mathbf{E}_{in} is not invertible, and its kernel has a dimension of one with $\mathbf{1}_M$ as its basis. Using the pseudo-inverse of this matrix to find \mathbf{c} yields a solution corresponding to the condition that $\sum c_k = 0$ following the construction of the invertible Loewner operator in Section III-A.1. From (9) and (10), we have the followings:

$$(\mathbf{E}_{\text{in}})_{rs} = \begin{cases} \frac{-2}{|\bar{z}_r - z_s|^2} & r \neq s \\ \sum_{k \neq r} \frac{2}{|\bar{z}_r - z_k|^2} & r = s \end{cases} \quad (15)$$

and

$$(\mathbf{F}_{\text{in}})_{rs} = \begin{cases} \frac{2}{|\bar{z}_r - z_s|^2} & r \neq s \\ \sum_{k \neq r} \frac{2}{|\bar{z}_r - z_k|^2} + \frac{4}{|\bar{z}_r - z_r|^2} & r = s. \end{cases} \quad (16)$$

Remark 6: In what follows, with a slight abuse of notation we will denote $L(\begin{bmatrix} \mathbf{a}^\top & \mathbf{b}^\top \end{bmatrix}^\top)$ with $L(\mathbf{a} + j\mathbf{b})$, and the same

convention is applied to L^{-*} . Additionally, if $L^{-1}(\mathbf{X}) = \begin{bmatrix} \mathbf{a}^\top & \mathbf{b}^\top \end{bmatrix}^\top$, then it is identified with the complex number $\mathbf{a} + j\mathbf{b}$. An analogous convention is adopted for L^* .

B. Initial Bound on the Identification Error

In this section, we first derive a preliminary bound on sample complexity (Lemma 2), which depends on a parameter called the minimum gain, ϕ , and includes a term that depends on noise. There is no analytical solution to (5), and thus it is not possible to explicitly compute $\hat{\mathbf{w}}$ to directly bound the sampled-frequency identification error $\|\hat{\mathbf{w}} - \bar{\mathbf{w}}\|_\infty$ by plugging in $\hat{\mathbf{w}}$. Nonetheless, a characterization of $\hat{\mathbf{w}}$ can be achieved through the optimality conditions of (5). The following Lemma provides a formal tool for this characterization:

Lemma 1: The vector $\hat{\mathbf{w}}$ is the optimal solution of (5) if and only if

$$\|L^{-*}\left(\sum_{s=1}^N (\tilde{\mathbf{w}}_s - \hat{\mathbf{w}})\right)\|_2 \leq \frac{\tau}{M}, \quad (17)$$

and

$$\left\langle \sum_{s=1}^N (\tilde{\mathbf{w}}_s - \hat{\mathbf{w}}), \hat{\mathbf{w}} \right\rangle = \frac{\tau}{M} \|L(\hat{\mathbf{w}})\|_*. \quad (18)$$

Proof: We apply the optimality conditions of Theorem 2 to (5). Define $f(\mathbf{x})$, $g(\mathbf{X})$, and L in (42) as

$$f(\mathbf{x}) = \frac{1}{2} \sum_{s=1}^N \|\mathbf{x} - \tilde{\mathbf{w}}_s\|_2^2, \quad g(\mathbf{X}) = \tau \frac{\|\mathbf{X}\|_*}{M},$$

with L being the Loewner operator. Consequently, $\hat{\mathbf{w}}$ is the optimal solution of (5) if and only if there exists $\mathbf{X} \in (\partial(\frac{\tau}{M} \|\cdot\|_*) \circ L)(\hat{\mathbf{w}})$ such that

$$-L^*(\mathbf{X}) = \sum_{s=1}^N (\hat{\mathbf{w}} - \tilde{\mathbf{w}}_s). \quad (19)$$

By the characterization of the subdifferential of nuclear norm (Proposition 2.1 in [58]), the inclusion $\mathbf{X} \in (\partial(\frac{\tau}{M} \|\cdot\|_*) \circ L)(\hat{\mathbf{w}})$ holds if and only if

$$\frac{M}{\tau} \langle \mathbf{X}, L(\hat{\mathbf{w}}) \rangle = \|L(\hat{\mathbf{w}})\|_*, \quad \|\mathbf{X}\|_2 \leq \frac{\tau}{M}. \quad (20)$$

Using the definition of the adjoint operator and (19), we rewrite the equality in (20) as

$$\begin{aligned} \frac{M}{\tau} \langle \mathbf{X}, L(\hat{\mathbf{w}}) \rangle &= \frac{M}{\tau} \langle L^*(\mathbf{X}), \hat{\mathbf{w}} \rangle \\ &= \frac{M}{\tau} \left\langle -\sum_{s=1}^N (\hat{\mathbf{w}} - \tilde{\mathbf{w}}_s), \hat{\mathbf{w}} \right\rangle \\ &= \|L(\hat{\mathbf{w}})\|_*. \end{aligned}$$

Thus, (20) is equivalent to

$$\left\langle \sum_{s=1}^N (\tilde{\mathbf{w}}_s - \hat{\mathbf{w}}), \hat{\mathbf{w}} \right\rangle = \frac{\tau}{M} \|L(\hat{\mathbf{w}})\|_*, \quad \|\mathbf{X}\|_2 \leq \frac{\tau}{M}. \quad (21)$$

Finally, solving for \mathbf{X} in (19) and substituting it into (21) completes the proof. \blacksquare

If we run only one experiment at each frequency ($N = 1$) and replace the Loewner operator L in (5) with the identity matrix,

then the LNNM problem reduces to a denoising problem. In this case, the objective is to recover a sparse vector from its noisy measurements. Motivated by this observation, we extend the approach in [59] to derive the sample complexity bounds for our setting. The next lemma establishes a preliminary upper bound on the sample complexity of our proposed method. This bound quantifies the identification error at a finite set of frequency points, specifically \mathbf{z} .

Lemma 2: Let the experimental frequency data be given as in (2) and (3). Denote by $\hat{\mathbf{w}}$ the system identified by solving the optimization problem (5). Then, the sampled-frequency identification error satisfies

$$\|\hat{\mathbf{w}} - \bar{\mathbf{w}}\|_\infty \leq \|\hat{\mathbf{w}} - \bar{\mathbf{w}}\|_2 \leq \frac{1}{\phi} \left(\frac{\tau}{MN} + \frac{\|\sum_{s=1}^N L^{-*}(\mathbf{v}_s)\|_2}{N} \right). \quad (22)$$

Here, ϕ denotes the *minimum gain* of the Loewner operator, defined as

$$\phi = \inf \left\{ \frac{\|\mathbf{u}\|_2}{\|L(\mathbf{u})\|_*} : \mathbf{u} \in T_{\bar{\mathbf{w}}} \right\}, \quad (23)$$

where $T_{\bar{\mathbf{w}}}$ is the following cone:

$$T_{\bar{\mathbf{w}}} = \{\mathbf{z} \in \mathbb{R}^n : \|L(\bar{\mathbf{w}} + \mathbf{z})\|_* \leq \|L(\bar{\mathbf{w}})\|_* + \alpha \|L(\mathbf{z})\|_*\},$$

with

$$\alpha = \frac{M}{\tau} \left\| \sum_{s=1}^N L^{-*}(\mathbf{v}_s) \right\|_2 \quad (24)$$

Proof: Write the square of the identification error as

$$\begin{aligned} \|\hat{\mathbf{w}} - \bar{\mathbf{w}}\|_2^2 &= \langle L(\hat{\mathbf{w}} - \bar{\mathbf{w}}), L^{-*}(\hat{\mathbf{w}} - \bar{\mathbf{w}}) \rangle \\ &= \langle L(\hat{\mathbf{w}} - \bar{\mathbf{w}}), L^{-*}(\hat{\mathbf{w}} - (\tilde{\mathbf{w}}_s - \mathbf{v}_s)) \rangle, \end{aligned}$$

where we used the definition of the adjoint operator to obtain the second equality and substituted $\bar{\mathbf{w}}$ with $\tilde{\mathbf{w}}_s - \mathbf{v}_s$ for the s^{th} experiment to derive the last expression. Summing over all experiments, we obtain

$$\begin{aligned} N \|\hat{\mathbf{w}} - \bar{\mathbf{w}}\|_2^2 &= \sum_{s=1}^N \langle L(\hat{\mathbf{w}} - \bar{\mathbf{w}}), L^{-*}(\hat{\mathbf{w}} - (\tilde{\mathbf{w}}_s - \mathbf{v}_s)) \rangle \\ &= \langle L(\hat{\mathbf{w}} - \bar{\mathbf{w}}), L^{-*} \left(\sum_{s=1}^N (\hat{\mathbf{w}} - (\tilde{\mathbf{w}}_s - \mathbf{v}_s)) \right) \rangle. \end{aligned}$$

By the definition of the dual norm, we have the inequality $\langle \mathbf{Z}, \mathbf{Y} \rangle \leq \|\mathbf{Z}\|_* \|\mathbf{Y}\|_2$, which leads to

$$\begin{aligned} N \|\hat{\mathbf{w}} - \bar{\mathbf{w}}\|_2^2 &\leq \|L(\hat{\mathbf{w}} - \bar{\mathbf{w}})\|_* \left\| L^{-*} \left(\sum_{s=1}^N (\hat{\mathbf{w}} - (\tilde{\mathbf{w}}_s - \mathbf{v}_s)) \right) \right\|_2 \\ &\leq \|L(\hat{\mathbf{w}} - \bar{\mathbf{w}})\|_* \left(\left\| L^{-*} \left(\sum_{s=1}^N (\hat{\mathbf{w}} - \tilde{\mathbf{w}}_s) \right) \right\|_2 \right. \\ &\quad \left. + \left\| L^{-*} \left(\sum_{s=1}^N \mathbf{v}_s \right) \right\|_2 \right), \end{aligned}$$

Utilizing the optimality condition (17) from Lemma 1, we deduce

$$N \|\hat{\mathbf{w}} - \bar{\mathbf{w}}\|_2^2 \leq \|L(\hat{\mathbf{w}} - \bar{\mathbf{w}})\|_* \left(\frac{\tau}{M} + \left\| L^{-*} \left(\sum_{s=1}^N \mathbf{v}_s \right) \right\|_2 \right).$$

Therefore, we conclude the following bound on $\|\hat{\mathbf{w}} - \bar{\mathbf{w}}\|_2$:

$$\|\hat{\mathbf{w}} - \bar{\mathbf{w}}\|_2 \leq \frac{\|L(\hat{\mathbf{w}} - \bar{\mathbf{w}})\|_*}{N \|\hat{\mathbf{w}} - \bar{\mathbf{w}}\|_2} \left(\frac{\tau}{M} + \left\| \sum_{s=1}^N L^{-*}(\mathbf{v}_s) \right\|_2 \right) \quad (25)$$

For the second part of the proof, we aim to exploit the definition of minimum gain. Since $\hat{\mathbf{w}}$ is the optimal solution of (5), it satisfies

$$\begin{aligned} \tau \frac{\|L(\hat{\mathbf{w}})\|_*}{M} + \frac{1}{2} \sum_{s=1}^N \|\hat{\mathbf{w}} - \tilde{\mathbf{w}}_s\|_2^2 \\ \leq \tau \frac{\|L(\bar{\mathbf{w}})\|_*}{M} + \frac{1}{2} \sum_{s=1}^N \|\bar{\mathbf{w}} - \tilde{\mathbf{w}}_s\|_2^2. \end{aligned}$$

Substituting $\tilde{\mathbf{w}}_s = \bar{\mathbf{w}} + \mathbf{v}_s$, we obtain

$$\begin{aligned} \tau \frac{\|L(\hat{\mathbf{w}})\|_*}{M} \\ \leq \tau \frac{\|L(\bar{\mathbf{w}})\|_*}{M} + \frac{1}{2} \sum_{s=1}^N \|\mathbf{v}_s\|_2^2 - \frac{1}{2} \sum_{s=1}^N \|\hat{\mathbf{w}} - \bar{\mathbf{w}} - \mathbf{v}_s\|_2^2 \\ \leq \tau \frac{\|L(\bar{\mathbf{w}})\|_*}{M} \\ \quad + \frac{1}{2} \sum_{s=1}^N \left(\|\mathbf{v}_s\|_2^2 - \langle \hat{\mathbf{w}} - \bar{\mathbf{w}} - \mathbf{v}_s, \hat{\mathbf{w}} - \bar{\mathbf{w}} - \mathbf{v}_s \rangle \right) \\ = \tau \frac{\|L(\bar{\mathbf{w}})\|_*}{M} + \frac{1}{2} \sum_{s=1}^N \left(-\|\hat{\mathbf{w}} - \bar{\mathbf{w}}\|_2^2 + 2\Re \langle \hat{\mathbf{w}} - \bar{\mathbf{w}}, \mathbf{v}_s \rangle \right) \\ \leq \tau \frac{\|L(\bar{\mathbf{w}})\|_*}{M} + \sum_{s=1}^N \Re \langle \hat{\mathbf{w}} - \bar{\mathbf{w}}, \mathbf{v}_s \rangle \\ = \tau \frac{\|L(\bar{\mathbf{w}})\|_*}{M} + \sum_{s=1}^N \Re \langle L(\hat{\mathbf{w}} - \bar{\mathbf{w}}), L^{-*}(\mathbf{v}_s) \rangle. \end{aligned}$$

Take the summation inside the inner product and utilize the definition of the dual norm to obtain

$$\begin{aligned} \tau \frac{\|L(\hat{\mathbf{w}})\|_*}{M} \\ \leq \tau \frac{\|L(\bar{\mathbf{w}})\|_*}{M} + \|L(\hat{\mathbf{w}} - \bar{\mathbf{w}})\|_* \left\| \sum_{s=1}^N L^{-*}(\mathbf{v}_s) \right\|_2 \\ = \tau \frac{\|L(\bar{\mathbf{w}})\|_*}{M} + \|L(\hat{\mathbf{w}} - \bar{\mathbf{w}})\|_* \left\| \sum_{s=1}^N L^{-*}(\mathbf{v}_s) \right\|_2, \end{aligned}$$

which leads to

$$\begin{aligned} \|L(\hat{\mathbf{w}})\|_* \\ \leq \|L(\bar{\mathbf{w}})\|_* + \frac{M \|\sum_{s=1}^N L^{-*}(\mathbf{v}_s)\|_2}{\tau} \|L(\hat{\mathbf{w}} - \bar{\mathbf{w}})\|_* \end{aligned}$$

This inequality implies that $\hat{\mathbf{w}} - \bar{\mathbf{w}}$ belongs to $T_{\bar{\mathbf{w}}}$ with $\alpha = \frac{M \|\sum_{s=1}^N L^{-*}(\mathbf{v}_s)\|_2}{\tau}$. Consequently, by the definition of ϕ in (23), we can bound the fraction $\frac{\|L(\hat{\mathbf{w}} - \bar{\mathbf{w}})\|_*}{\|\hat{\mathbf{w}} - \bar{\mathbf{w}}\|_2}$ in (25) from above by $\frac{1}{\phi}$. This yields (22), completing the proof. \blacksquare

Remark 7: Ensuring $\alpha < 1$ is essential for the validity of the minimum gain argument. When $\alpha = 0$, the cone $T_{\bar{\mathbf{w}}}$ contains exactly the directions along which the nuclear norm of the Loewner matrix decreases, which is desirable since

our goal is to recover a low-order system. However, deriving a bound for the case $\alpha = 0$ is not possible here, as the optimization in (5) jointly minimizes not only the nuclear norm of the Loewner matrix but also the squared distance between the measured and predicted frequency responses. For this reason, the cone must be widened by allowing $\alpha > 0$. Nonetheless, if $\alpha = 1$, the inequality becomes trivial and the directions in $T_{\bar{\mathbf{w}}}$ no longer represent descent directions for minimizing the nuclear norm. Thus, keeping α strictly less than one is important. Later, in the proof of Theorem 1, we will show that choosing τ optimally ensures $\alpha < 1$.

Remark 8: An examination of (22) reveals a conceptual resemblance to the classical bias-variance tradeoff in machine learning [60]. In this formulation, the first term represents the bias, regulated by the parameter τ , which steers the model toward low-order systems. The second term is analogous to the variance, arising from the presence of noise in the data.

C. Bounding the Minimum Gain

Next, we derive a lower bound on the minimum gain of the Loewner operator when acting over the elements of a suitably defined cone. To this end, let Assumptions 1 and 3 hold. Consider the singular value decomposition of the Loewner matrix constructed from the true frequency response:

$$L(\bar{\mathbf{w}}) = [\mathbf{U}_1 \quad \dots] \begin{bmatrix} \Sigma_1 & \mathbf{0} \\ \mathbf{0} & \mathbf{0} \end{bmatrix} [\mathbf{V}_1 \quad \dots]^* = \mathbf{U}_1 \Sigma_1 \mathbf{V}_1^*,$$

where Σ_1 is of dimension κ , representing the true order of the system.

We adopt the projection technique widely used in the literature [59], [61]–[64]. Define the subspace

$$T = \{ \mathbf{U}_1 \mathbf{X} + \mathbf{Y} \mathbf{V}_1^* : \mathbf{X} \in \mathbb{C}^{\kappa \times M}, \mathbf{Y} \in \mathbb{C}^{M \times \kappa} \},$$

which corresponds to the tangent space, at $L(\bar{\mathbf{w}})$, to the manifold of matrices of rank κ . The orthogonal subspace to T is

$$T^\perp = \{ \mathbf{Z} \in \mathbb{C}^{M \times M} : \mathbf{U}_1^* \mathbf{Z} = \mathbf{0}_{\kappa \times M}, \mathbf{Z} \mathbf{V}_1 = \mathbf{0}_{M \times \kappa} \}.$$

The projection operators onto these subspaces are given by

$$\begin{aligned} \mathcal{P}(\mathbf{X}) &= \mathbf{U}_1 \mathbf{U}_1^* \mathbf{X} + \mathbf{X} \mathbf{V}_1 \mathbf{V}_1^* - \mathbf{U}_1 \mathbf{U}_1^* \mathbf{X} \mathbf{V}_1 \mathbf{V}_1^*, \\ \mathcal{P}^\perp(\mathbf{X}) &= (\mathbf{I}_M - \mathbf{U}_1 \mathbf{U}_1^*) \mathbf{X} (\mathbf{I}_M - \mathbf{V}_1 \mathbf{V}_1^*). \end{aligned}$$

Let $\mathbf{u} \in T_{\bar{\mathbf{w}}}$, that is

$$\|L(\bar{\mathbf{w}} + \mathbf{u})\|_* \leq \|L(\bar{\mathbf{w}})\|_* + \alpha \|L(\mathbf{u})\|_*.$$

By the linearity of the Loewner operator, this simplifies to

$$\|L(\bar{\mathbf{w}}) + L(\mathbf{u})\|_* \leq \|L(\bar{\mathbf{w}})\|_* + \alpha \|L(\mathbf{u})\|_*. \quad (26)$$

On the other hand, decompose $L(\mathbf{u})$ as $L(\mathbf{u}) = \mathcal{P}(L(\mathbf{u})) + \mathcal{P}^\perp(L(\mathbf{u}))$, and write the singular value decomposition $\mathcal{P}^\perp(L(\mathbf{u})) = \mathbf{U}_2 \Sigma_2 \mathbf{V}_2^* \in T^\perp$. From the characterization of the subdifferential of the nuclear norm [65], we have

$$\partial \|\cdot\|_*(L(\bar{\mathbf{w}})) = \{ \mathbf{U}_1 \mathbf{V}_1^* + \mathbf{Z} : \mathbf{Z} \in T^\perp, \|\mathbf{Z}\|_2 \leq 1 \}.$$

Let $\mathbf{H} = \mathbf{U}_2 \mathbf{V}_2^*$. Then $\mathbf{H} \in T^\perp$ and $\|\mathbf{H}\|_2 = 1$. Therefore, $\mathbf{U}_1 \mathbf{V}_1^* + \mathbf{H}$ is a valid subgradient at $L(\bar{\mathbf{w}})$, which implies

$$\begin{aligned} \|L(\bar{\mathbf{w}}) + L(\mathbf{u})\|_* &\geq \|L(\bar{\mathbf{w}})\|_* + \langle \mathbf{U}_1 \mathbf{V}_1^* + \mathbf{H}, L(\mathbf{u}) \rangle \\ &= \|L(\bar{\mathbf{w}})\|_* + \langle \mathbf{U}_1 \mathbf{V}_1^* + \mathbf{H}, \mathcal{P}(L(\mathbf{u})) + \mathcal{P}^\perp(L(\mathbf{u})) \rangle. \end{aligned} \quad (27)$$

We expand the inner product:

$$\begin{aligned} &\langle \mathbf{U}_1 \mathbf{V}_1^*, \mathcal{P}(L(\mathbf{u})) \rangle + \langle \mathbf{U}_1 \mathbf{V}_1^*, \mathcal{P}^\perp(L(\mathbf{u})) \rangle \\ &\quad + \langle \mathbf{H}, \mathcal{P}(L(\mathbf{u})) \rangle + \langle \mathbf{H}, \mathcal{P}^\perp(L(\mathbf{u})) \rangle. \end{aligned}$$

The first term satisfies

$$|\langle \mathbf{U}_1 \mathbf{V}_1^*, \mathcal{P}(L(\mathbf{u})) \rangle| \leq \|\mathbf{U}_1 \mathbf{V}_1^*\|_2 \|\mathcal{P}(L(\mathbf{u}))\|_* = \|\mathcal{P}(L(\mathbf{u}))\|_*.$$

The second and third terms vanish due to orthogonality, and the last term is

$$\text{Tr}((\mathbf{U}_2 \mathbf{V}_2^*)^* \mathbf{U}_2 \Sigma_2 \mathbf{V}_2^*) = \text{Tr}(\mathbf{V}_2 \Sigma_2 \mathbf{V}_2^*) = \|\mathcal{P}^\perp(L(\mathbf{u}))\|_*.$$

Substituting these four terms into (27) yields

$$\|L(\bar{\mathbf{w}}) + L(\mathbf{u})\|_* \geq \|L(\bar{\mathbf{w}})\|_* - \|\mathcal{P}(L(\mathbf{u}))\|_* + \|\mathcal{P}^\perp(L(\mathbf{u}))\|_*.$$

Now substitute this lower bound into (26) to obtain

$$\begin{aligned} \|L(\bar{\mathbf{w}})\|_* - \|\mathcal{P}(L(\mathbf{u}))\|_* + \|\mathcal{P}^\perp(L(\mathbf{u}))\|_* \\ \leq \|L(\bar{\mathbf{w}})\|_* + \alpha \|L(\mathbf{u})\|_* \\ \leq \|L(\bar{\mathbf{w}})\|_* + \alpha \|\mathcal{P}(L(\mathbf{u}))\|_* + \alpha \|\mathcal{P}^\perp(L(\mathbf{u}))\|_*. \end{aligned}$$

The cancellation of $\|L(\bar{\mathbf{w}})\|_*$ and the rearranging of terms gives

$$(1 - \alpha) \|\mathcal{P}^\perp(L(\mathbf{u}))\|_* \leq (1 + \alpha) \|\mathcal{P}(L(\mathbf{u}))\|_*. \quad (28)$$

In addition, we have

$$\begin{aligned} \|L(\mathbf{u})\|_* &\leq \|\mathcal{P}(L(\mathbf{u}))\|_* + \|\mathcal{P}^\perp(L(\mathbf{u}))\|_* \\ &\leq \frac{2}{1 - \alpha} \|\mathcal{P}(L(\mathbf{u}))\|_*, \end{aligned}$$

where we used (28) to derive the last inequality. By the relationship between the nuclear norm and the Frobenius norm, given by $\|\mathbf{X}\|_* \leq \sqrt{\text{Rank}(\mathbf{X})} \|\mathbf{X}\|_F$, we obtain

$$\begin{aligned} \|L(\mathbf{u})\|_* &\leq \frac{2}{1 - \alpha} \|\mathcal{P}(L(\mathbf{u}))\|_* \\ &\leq \frac{2\sqrt{2\kappa}}{1 - \alpha} \|\mathcal{P}(L(\mathbf{u}))\|_F \leq \frac{2\sqrt{2\kappa}}{1 - \alpha} \|L(\mathbf{u})\|_F, \end{aligned} \quad (29)$$

where we used that $\text{rank}(\mathcal{P}(X)) \leq 2\kappa$ for $X \in \mathbb{C}^{M \times M}$ because $\mathcal{P}(X) = \mathbf{U}_1 \mathbf{U}_1^* X + X \mathbf{V}_1 \mathbf{V}_1^* - \mathbf{U}_1 \mathbf{U}_1^* X \mathbf{V}_1 \mathbf{V}_1^*$ with $\text{rank}(\mathbf{U}_1) = \text{rank}(\mathbf{V}_1) = \kappa$, and that $\|\mathcal{P}(\mathbf{X})\|_F \leq \|\mathbf{X}\|_F$ for any orthogonal projector \mathcal{P} . Applying Lemma 4 to bound $\|L(\mathbf{u})\|_F$, we have for sufficiently large M

$$\|L(\mathbf{u})\|_* \leq \frac{2\sqrt{2\kappa}}{1 - \alpha} 3 \sqrt{1 + \frac{2K}{\rho - 1} \frac{\sqrt{-M \ln \sin \delta_m}}{\pi - 2\delta_m}} \|\mathbf{u}\|_2.$$

Rearranging the terms, we obtain

$$\frac{\|\mathbf{u}\|_2}{\|L(\mathbf{u})\|_*} \geq \frac{(1 - \alpha)(\pi - 2\delta_m)}{6 \sqrt{1 + \frac{2K}{\rho - 1} \sqrt{-2\kappa M \ln \sin \delta_m}}}.$$

Finally, since ϕ is the infimum of the LHS over all $\mathbf{u} \in T_{\bar{w}}$, we derive the following lower bound for the minimum gain:

$$\phi \geq \frac{(1-\alpha)(\pi-2\delta_m)}{6\sqrt{1+\frac{2K}{\rho-1}}\sqrt{-2\kappa M \ln \sin \delta_m}}. \quad (30)$$

Remark 9: Note that the inequality (29) can be replaced by the trivial bound $\|L(\mathbf{u})\|_* \leq \sqrt{M}\|L(\mathbf{u})\|_F$, and depending on the value of α , this trivial bound could be sharper. Thus, a better approach is to use the inequality

$$\|L(\mathbf{u})\|_* \leq \min \left\{ \frac{2\sqrt{2\kappa}}{1-\alpha}, \sqrt{M} \right\} \|L(\mathbf{u})\|_F.$$

Nonetheless, we choose only the κ -dependent bound since we are interested in the dependence of the sample complexity bound in the regime where M is large, while κ is small because the underlying system is assumed to be of low order. In other words, the final dependence of the sample complexity in big- \mathcal{O} notation will not be affected by this choice, as for large M the term $\min \left\{ \frac{2\sqrt{2\kappa}}{1-\alpha}, \sqrt{M} \right\}$ reduces to $\frac{2\sqrt{2\kappa}}{1-\alpha}$.

D. Bounding the Noise-Dependent Term

Finally, to complete the derivation of the sample complexity's bound, we establish an upper bound on the maximum error associated with the inverse adjoint of the Loewner operator of the noise: $\|L^{-1}(\mathbf{v}_s)\|_2$. To this end, let Assumptions 2 and 3 hold. Recall the explicit formula for the inverse adjoint Loewner operator from (14):

$$\begin{aligned} L^{-*}(\mathbf{v}_s) &= L^{-*} \left(\begin{bmatrix} \mathbf{a}_s \\ \mathbf{b}_s \end{bmatrix} \right) \\ &= \sum_{k=1}^M \left(\mathbf{e}_k^\top \mathbf{E}_{\text{in}}^\dagger \mathbf{a}_s \mathbf{E}_k \right) + \sum_{k=1}^M \left(\mathbf{e}_k^\top \mathbf{F}_{\text{in}}^{-1} \mathbf{b}_s \mathbf{F}_k \right). \end{aligned} \quad (31)$$

To upper bound $\|L^{-*}(\mathbf{v}_s)\|_2$, we derive lower bounds on the smallest singular values of the matrices \mathbf{E}_{in} and \mathbf{F}_{in} ⁴. These matrices exhibit a specific structure, allowing us to establish a lower bound on their minimum nonzero singular values as follows:

For the matrix \mathbf{E}_{in} , examining (15) reveals that it is the Laplacian matrix of a graph. This observation aligns with the fact that its null space is one-dimensional, with $\mathbf{1}_M$ being the associated eigenvector. Furthermore, each entry of \mathbf{E}_{in} has an absolute value of at least 0.5. Consequently, by applying Lemma 5, we establish that the algebraic connectivity, defined as the smallest nonzero eigenvalue, of \mathbf{E}_{in} (in this case: $\lambda_{M-1}(\mathbf{E}_{\text{in}})$) is at least $M/2$. As a result, we obtain the bound

$$\|\mathbf{E}_{\text{in}}^\dagger\|_2 \leq \frac{2}{M}. \quad (32)$$

Consider a term in the first summation in the RHS of (31): $\mathbf{e}_k^\top \mathbf{E}_{\text{in}}^\dagger \mathbf{a}_s \mathbf{E}_k$. We may bound this term as follows

$$\begin{aligned} \|\mathbf{e}_k^\top \mathbf{E}_{\text{in}}^\dagger \mathbf{a}_s \mathbf{E}_k\|_2 &\leq |\mathbf{e}_k^\top \mathbf{E}_{\text{in}}^\dagger \mathbf{a}_s| \|\mathbf{E}_k\|_2 \\ &\leq \|\mathbf{E}_{\text{in}}^\dagger\|_2 \|\mathbf{a}_s\|_2 \|\mathbf{E}_k\|_2 \leq \frac{2\bar{\eta}}{M} \|\mathbf{E}_k\|_F \end{aligned} \quad (33)$$

⁴Since \mathbf{E}_{in} and \mathbf{F}_{in} are positive semidefinite matrices, their eigenvalues and singular values are identical.

in which we used (32), Assumption 2, and the relation $\|\cdot\|_2 \leq \|\cdot\|_F$ to conclude the last inequality.

For the matrix \mathbf{F}_{in} , examining (16) reveals that we can decompose it as

$$\mathbf{F}_{\text{in}} = \mathbf{G}_{\text{in}} + \mathbf{D}_{\text{in}}$$

in which $(\mathbf{G}_{\text{in}})_{rs} = \frac{2}{|\bar{z}_r - z_s|^2}$ and \mathbf{D}_{in} is a diagonal matrix such that $(\mathbf{D}_{\text{in}})_{rr} = \sum_k \left(\frac{2}{|\bar{z}_r - z_k|^2} \right)$. Lemma 6 which follows from Theorem 4 proves that \mathbf{G}_{in} is positive definite. Therefore,

$$\begin{aligned} \lambda_{\min}(\mathbf{F}_{\text{in}}) &\geq \lambda_{\min}(\mathbf{D}_{\text{in}}) = \min_r D_{rr} \\ &= \min_r \sum_k \left(\frac{2}{|\bar{z}_r - z_k|^2} \right) \geq \sum_k \frac{2}{4} = \frac{M}{2}, \end{aligned}$$

where we used $|\bar{z}_r - z_k| \leq 2$ to derive the second inequality. Consequently, $\|\mathbf{F}_{\text{in}}^{-1}\|_2 \leq \frac{2}{M}$. Similar to (33), we may bound a term in the second summation in the RHS of (31), $\mathbf{e}_k^\top \mathbf{F}_{\text{in}} \mathbf{b}_s \mathbf{F}_k$, as follows

$$\|\mathbf{e}_k^\top \mathbf{F}_{\text{in}} \mathbf{b}_s \mathbf{F}_k\|_2 \leq \frac{2\bar{\eta}}{M} \|\mathbf{F}_k\|_F. \quad (34)$$

We aim to apply Theorem 3 to $\sum_{s=1}^N L^{-*}(\mathbf{v}_s)$. In this case, we may choose \mathbf{A}_k in Theorem 3 to be $\frac{2\bar{\eta}}{M} \|\mathbf{E}_k\|_F \mathbf{I}_M$ and $\frac{2\bar{\eta}}{M} \|\mathbf{F}_k\|_F \mathbf{I}_M$ for the first and second summations in (31). Thus, the variance σ^2 in Theorem 3 is:

$$\begin{aligned} \sigma^2 &= \left\| \sum_{s=1}^N \sum_{k=1}^M \frac{4\bar{\eta}^2}{M^2} \|\mathbf{E}_k\|_F^2 \mathbf{I}_M + \sum_{k=1}^M \frac{4\bar{\eta}^2}{M^2} \|\mathbf{F}_k\|_F^2 \mathbf{I}_M \right\|_2 \\ &= \frac{4N\bar{\eta}^2}{M^2} \sum_{k=1}^M (\|\mathbf{E}_k\|_F^2 + \|\mathbf{F}_k\|_F^2) \\ &= \frac{4N\bar{\eta}^2}{M^2} \sum_{k=1}^M \left(\sum_{s \neq k} \frac{2}{|\bar{z}_k - z_s|^2} + \right. \\ &\quad \left. \sum_{s \neq k} \frac{2}{|\bar{z}_k - z_s|^2} + \frac{4}{|\bar{z}_k - z_k|^2} \right) \\ &= \frac{16N\bar{\eta}^2}{M^2} \sum_{k=1}^M \sum_{s=1}^M \frac{1}{|\bar{z}_k - z_s|^2}. \end{aligned}$$

Consequently by the application of Lemma 7, σ is bounded by:

$$\sigma \leq \frac{4\bar{\eta}\sqrt{-2N \ln \sin \delta_m}}{\pi - 2\delta_m}.$$

Surprisingly, σ does not depend on M . Finally, by choosing $t = 2\sqrt{2}\sigma\sqrt{\ln(\frac{M}{\delta})}$ in (44), we obtain

$$\begin{aligned} \mathbb{P} \left(\left\| \sum_{s=1}^N L^{-*}(\mathbf{v}_s) \right\|_2 \geq \right. \\ \left. \frac{16\bar{\eta}\sqrt{-N \ln(\sin(\delta_m)) \ln(\frac{M}{\delta})}}{\pi - 2\delta_m} \right) \leq \delta. \end{aligned} \quad (35)$$

E. Sampled-Frequency Identification Error

The following theorem states one of our main results: a bound on the sampled-frequency identification error for the LNNM algorithm (5):

Theorem 1: Let the experimental frequency data be given as in (2) and denote by $\hat{\mathbf{w}}$ the system identified by solving the optimization problem (5). Provided that assumptions 1, 2, and 3 hold, the sampled-frequency identification error satisfies, with probability at least $1 - \delta$,

$$\|\hat{\mathbf{w}} - \bar{\mathbf{w}}\|_\infty \leq 96(1 + \sqrt{2})^2 \sqrt{2\kappa} \sqrt{1 + \frac{2K}{\rho-1} \bar{\eta} \frac{(-\ln \sin \delta_m)}{(\pi - 2\delta_m)^2}} \sqrt{\frac{M \ln(\frac{M}{\delta})}{N}} \quad (36)$$

in which κ is the true order of the system.

Proof: By substituting ϕ from (30) and the bound from (35) into (22), we derive the following sample complexity bound as a consequence of Lemma 2:

$$\begin{aligned} \|\hat{\mathbf{w}} - \bar{\mathbf{w}}\|_\infty \leq & \frac{6\sqrt{2\kappa} \sqrt{1 + \frac{2K}{\rho-1}}}{(1-\alpha)(\pi - 2\delta_m)} \left(\frac{\tau}{N} \sqrt{\frac{-\ln \sin \delta_m}{M}} \right. \\ & \left. + \frac{-16\bar{\eta} \ln \sin \delta_m \sqrt{M \ln(\frac{M}{\delta})}}{(\pi - 2\delta_m) \sqrt{N}} \right). \end{aligned} \quad (37)$$

Next, using the bound in (35) we can upper bound α given in (24) as:

$$\alpha \leq \frac{M}{\tau} \frac{16\bar{\eta} \sqrt{-N \ln(\sin(\delta_m)) \ln(\frac{M}{\delta})}}{\pi - 2\delta_m} \quad (38)$$

The substitution of this bound into (37) removes the dependency on α and yields an expression of the form $D \frac{A\tau+B}{1-\frac{C}{\tau}}$, where A , B , C , and D are independent of τ . This bound attains its minimum at $\tau^* = C + \sqrt{C^2 + \frac{CB}{A}}$ resulting in

$$\tau^* = (1 + \sqrt{2}) \frac{16\bar{\eta} M \sqrt{-N \ln(\sin(\delta_m)) \ln(\frac{M}{\delta})}}{\pi - 2\delta_m}. \quad (39)$$

Interestingly, substitution of this optimal τ^* into (38) yields the bound $\alpha \leq \sqrt{2} - 1 < 1$. Finally, substitution of $\tau = \tau^*$ and $\alpha = \sqrt{2} - 1$ into (37) yields the final bound. ■

Remark 10: The sample complexity bound derived in (36) exhibits a convergence rate of $\mathcal{O}(N^{-1/2})$, which aligns with the general expectations for identification errors. When logarithmic factors are disregarded, the dependency on the number of frequency points is $\mathcal{O}(M^{1/2})$, which is analogous to the bound derived in [43] for the empirical transfer function estimate. In that work, the frequency points correspond to a fixed grid used in the Fourier transform, with data acquired in the time domain under specific excitation conditions. Lastly, the linear dependency on the noise level $\mathcal{O}(\bar{\eta})$ is consistent with the bound derived in [66] for model order reduction in the Loewner framework, albeit under a Gaussian noise assumption.

F. Bounding the Identification Error Over all Frequencies.

In the previous section, we derived a bound on the identification error over a fixed set of frequencies. To extend this result to all frequencies, we treat these fixed frequencies as interpolation points and derive a bound, in the \mathcal{H}_∞ sense, on the identification error, assuming that system is estimated using an interpolation-based method [67].

Corollary 1: If an interpolation based algorithm is used to identify \hat{G} from its sampled frequency response obtained solving (5) and assumptions 1, 2, and 3 hold, then with probability at least $1 - \delta$ the following bound holds

$$\|\hat{G} - \bar{G}\|_\infty \leq 2 \frac{\epsilon + K\psi(\bar{\delta})}{1 + \frac{\epsilon}{K}\psi(\bar{\delta})} \quad (40)$$

where ϵ is the RHS of (36) and

$$\psi(\bar{\delta}) = \frac{2\rho \sin(\frac{\bar{\delta}}{2})}{\sqrt{(\rho^2 - 1)^2 + 4\rho^2 \sin^2(\frac{\bar{\delta}}{2})}}.$$

$\bar{\delta}$ is the maximum arc distance between each pair in $[\mathbf{z}^\top \bar{\mathbf{z}}^\top]^\top$.

Proof: The proof is a direct consequence of Theorem 5.2 in [67] and Theorem 1. ■

Remark 11: The number of frequency points, M , influences the identification error in (40) through both ϵ and $\bar{\delta}$. In the case of equally spaced points \mathbf{z} , $\bar{\delta}$ is given by $\max\{2\delta_m + \frac{\pi}{M}, \pi/M\}$. Consequently, as M increases, $\psi(\bar{\delta})$ decreases at a rate of $\mathcal{O}(1/M)$ until $\frac{\pi}{M}$ falls below $2\delta_m + \frac{\pi}{M}$. Beyond this threshold, $\psi(\bar{\delta})$ remains almost constant: $2\delta_m$, and thus the error scales according to the ϵ term. Overall, for sufficiently large M , the identification error scales in the same manner as the bound derived in Theorem 1.

IV. NUMERICAL EXAMPLE

In this section, we present numerical experiments to validate our main results.⁵ Section IV-A highlights how our approach promotes low-order representations, and Section IV-B validates the sample complexity bound. For experiments, we use the following system from [43] as the ground-truth model:

$$G(z) = \frac{0.12z + 0.18z^2}{1 - 1.4z^1 + 1.443z^2 - 1.123z^3 + 0.7729z^4}. \quad (41)$$

A. Low-order identification

The classical approach to estimate the frequency response from empirical frequency-domain data involves averaging measurements from multiple experiments at each frequency and then proceeding to obtain a realization using any system identification method such as Loewner interpolation [51]. This approach is equivalent to solving (5) with $\tau = 0$, followed by interpolation in the Loewner framework. In this experiment, we demonstrate that the solution of (5) with an appropriately chosen regularization parameter can effectively promote low-order representations. As previously discussed, while the sample complexity bound was derived under Assumptions 1,

⁵Code available at https://github.com/Arya-Honarparisheh/freq_iden_low_order.

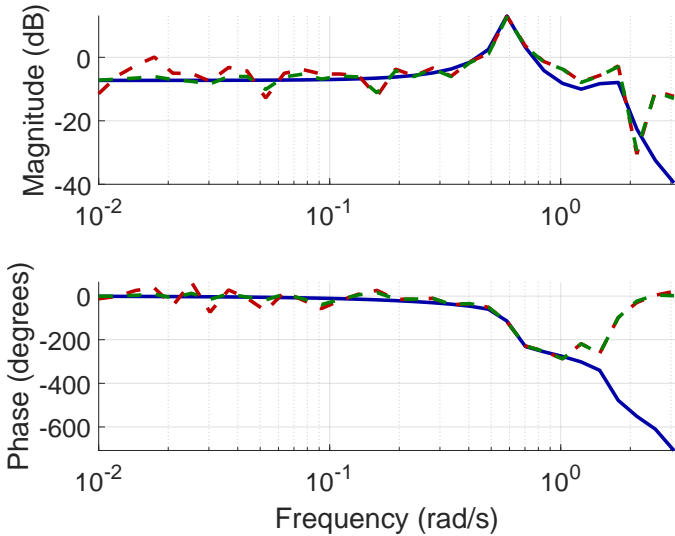


Fig. 2. *Bode Diagrams*: The solid blue line represents the frequency response of the [ground truth system](#). The frequency responses of the systems identified by [Averaging](#) and [LNNM](#) are represented by red and green dashed lines, respectively. It is observed that at low frequencies, LNNM exhibits less fluctuation, resulting in a response that is closer to the baseline.

2, and 3, these assumptions are not strictly required for the implementation of the proposed method. Thus, our experiments were conducted using $M = 32$ logarithmically spaced frequencies to enhance the resolution of high-frequency behavior, and the number of experiments at each frequency was set to $N = 30$. The measurement noise was generated as a uniformly distributed random variable bounded by $\bar{\eta} = 2$, and the regularization parameter was set to $\tau = 20$. Note that the regularization parameter in (39) is optimal only with respect to the upper bound in (38). Since this bound may be loose, in practice we tune τ by trial-and-error or cross-validation.

Figure 2 compares the estimated frequency responses using averaging and LNNM to the baseline, which corresponds to the frequency response of the system given in (41). Figure 3 compares the \mathcal{H}_∞ identification error of the averaging method and LNNM, demonstrating that solving (5) leads to a lower identification error. Finally, Figure 4 highlights the effectiveness of the proposed method by comparing the singular values of the corresponding Loewner matrices. Note that, due to process noise, averaging increases the Hankel singular values of the resulting model. On the other hand, by minimizing the nuclear norm, LNNM yields a lower order system closer to the ground truth.

B. Numerical verification of Sample Complexity

In this section, we examine the dependency of the sample complexity bound in (36) with respect to N , M , and $\bar{\eta}$. Monte Carlo simulations comprising 20 independent experiments were conducted to analyze the dependency of the \mathcal{H}_∞ identification error. Figures 5, 6, and 7 present plots of the \mathcal{H}_∞ identification error versus N , M , and $\bar{\eta}$, respectively.

In all experiments, we set $N = 30$, $M = 32$, and $\bar{\eta} = 0.5$, unless the respective variable appears as the independent variable on the horizontal axis. The measurement noise

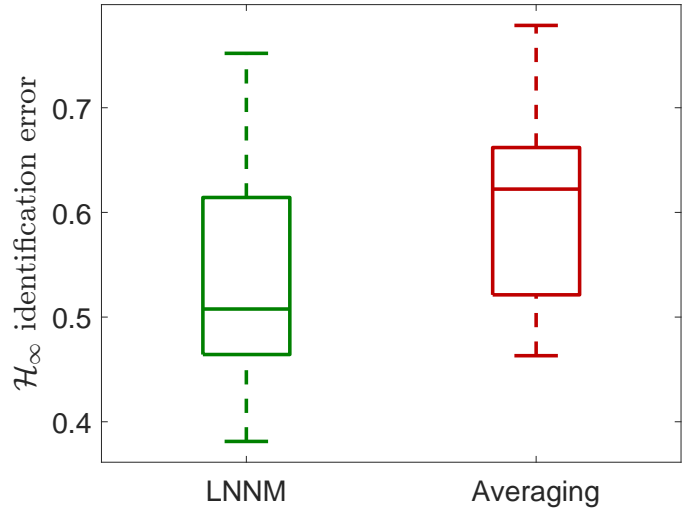


Fig. 3. *\mathcal{H}_∞ Identification Error*: The \mathcal{H}_∞ identification error of the proposed [LNNM](#) method is compared with that of the [Averaging](#) approach, in which the N frequency response measurements at each frequency are averaged. A Monte Carlo simulation was performed by repeating the experiment 20 times for a fair comparison.

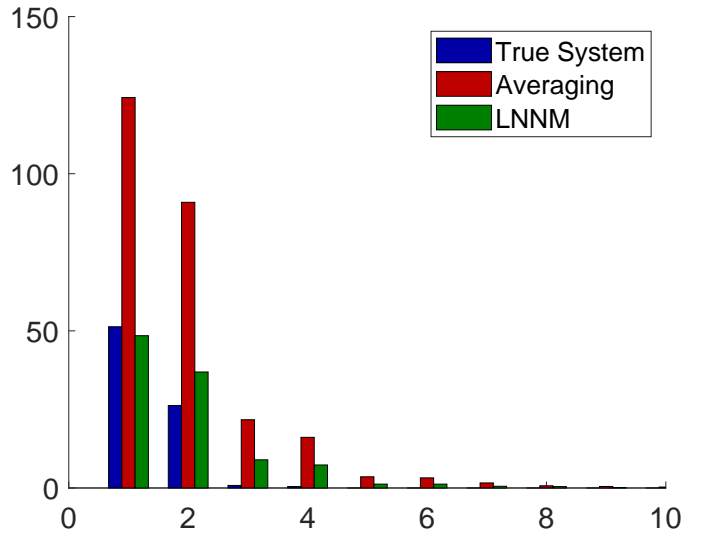


Fig. 4. *Singular Values of Loewner Matrix*: The decay of the singular values indicates that the system identified using [Averaging](#) has a higher order, whereas the system identified using [LNNM](#) is of lower order and closer to the low-order [ground truth system](#).

was generated as a uniformly distributed, bounded random variable, in accordance with Assumption 2. The frequency points were equally spaced, with the frequency margin set to $\delta_m = 0.1$ to be consistent with Assumption 3. Additionally, Assumption 1 holds, as the system defined in (41) is stable. Finally, the regularization parameter was set to $\tau = 7$.

V. CONCLUSIONS

The past few years have seen a renewed interest in identification methods based on regularized optimization. In the case of time domain data, this research has led to non-asymptotic sample complexity bounds. However, a similar analysis for the frequency domain is not available. In this paper, we propose an alternative, frequency-domain-based system identification

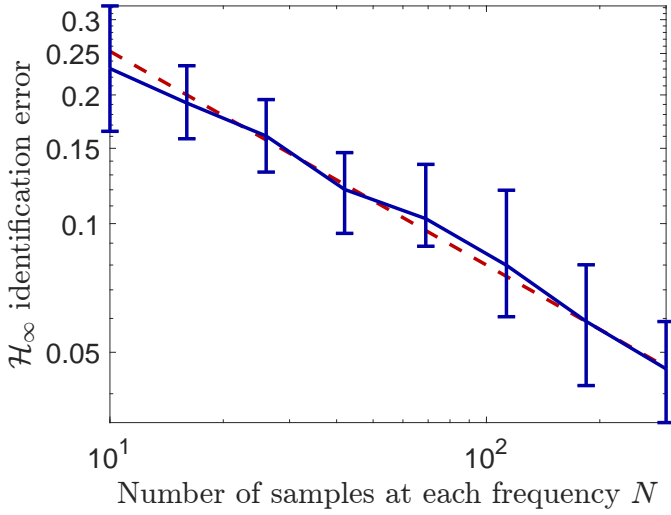


Fig. 5. \mathcal{H}_∞ Identification Error as a Function of N : The results are presented in a logarithmic scale, where the red dotted line represents a reference slope of 0.5, confirming the $\mathcal{O}(N^{-\frac{1}{2}})$ scaling in sample complexity.

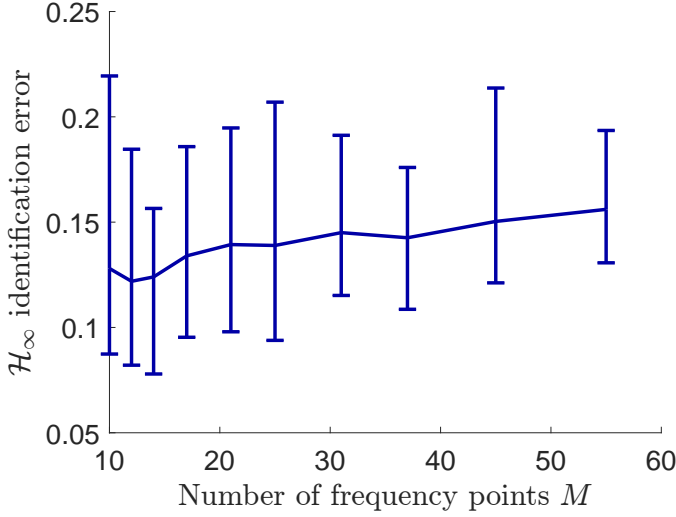


Fig. 6. \mathcal{H}_∞ Identification Error as a Function of M : As shown in the graph, the dependency does not increase rapidly with M , leading to the conjecture that the theoretical growth rate $\mathcal{O}((M \ln M)^{\frac{1}{2}})$ may not be sharp enough and could potentially be refined through a more detailed analysis.

method for learning low-order systems. The identification problem is formulated as the minimization of the ℓ_2 norm between the identified and measured frequency responses, with the nuclear norm of the Loewner matrix serving as a regularization term. Our main result provides an upper bound on the sample complexity of the identification process, shedding light on the different factors that affect it. Specifically, we establish that the sample complexity of the identification error scales as $\mathcal{O}(\sqrt{\frac{M \ln M}{N}})$. To the best of our knowledge, this is the first non-asymptotic bound for the regularization-based frequency-domain algorithms. The efficacy of the proposed method in obtaining a low-order model was demonstrated through an example, along with numerical simulations validating the growth rate of the sample complexity bound. Notably, as indicated

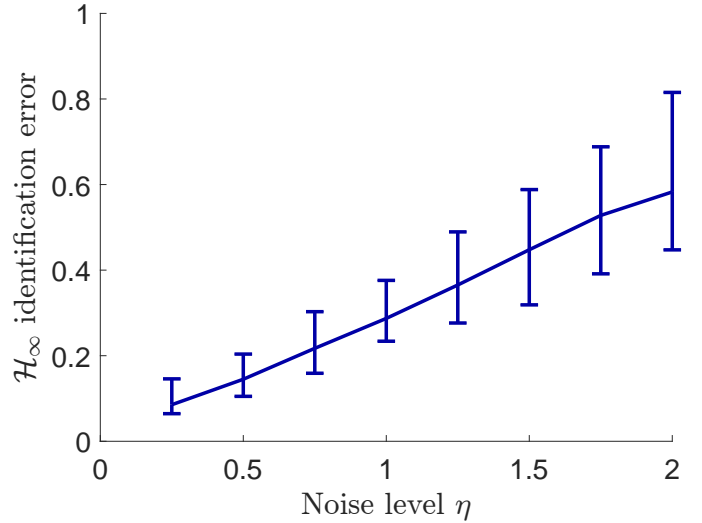


Fig. 7. \mathcal{H}_∞ Plot of the Identification Error as a Function of $\bar{\eta}$ illustrating the linear dependency on the noise level, $\mathcal{O}(\bar{\eta})$.

by Fig. 6, the bound on the growth of the sample complexity with M may be conservative. Future research involves deriving sharper bounds and relaxing our assumptions. Additionally, the proposed method can be adopted in applications where frequency-related system properties are the main objective, providing an alternative to the time-domain approaches used in those applications [68], [69].

APPENDIX I TECHNICAL BACKGROUNDS

A. Optimality Condition

In our analysis, we must characterize the solution of a convex minimization problem. Optimality conditions—such as Fermat’s rule or the Karush-Kuhn-Tucker (KKT) conditions—provide the necessary tools for this purpose. In particular, we rely on the following generalized form of Fermat’s rule.

Theorem 2 ([70] Theorem 27.2): Assume \mathcal{H} and \mathcal{K} are finite-dimensional Hilbert spaces. Let $f : \mathcal{H} \rightarrow \mathbb{R}$ and $g : \mathcal{K} \rightarrow \mathbb{R}$ be closed proper convex functions. Let $L : \mathcal{H} \rightarrow \mathcal{K}$ be a linear operator. Consider the following optimization problem:

$$\min_{x \in \mathcal{H}} f(x) + g(L(x)). \quad (42)$$

Then \hat{x} is the optimal solution of (42) iff

$$\exists v \in \partial g(L\hat{x}) \text{ such that } -L^*v \in \partial f(\hat{x}). \quad (43)$$

B. Concentration of Measure

Probability Approximately Correct (PAC) bounds in system identification provide valuable information on the capabilities and limitations of learning algorithms [71]. Concentration inequalities serve as powerful tools for establishing such bounds. Under reasonable assumptions regarding the distribution of noise, it is possible to analyze how certain random variables, such as the identification error, which depends on the noise distribution, concentrate around a specific value. The following

theorem presents a matrix Hoeffding concentration inequality, which we later exploit in our analysis:

Theorem 3 (Theorem 1.3 from [72]): Consider a finite sequence $\{\mathbf{X}_s\}_{s=1}^N$ of independent, random, self-adjoint matrices with dimension M , and let $\{\mathbf{A}_s\}_{s=1}^N$ be a sequence of fixed self-adjoint matrices. Assume that each random matrix satisfies $\mathbb{E}(\mathbf{X}_s) = \mathbf{0}$ and $\mathbf{A}_s^2 - \mathbf{X}_s^2 \succeq 0$ almost surely. Then, for all $t \geq 0$,

$$\mathbb{P} \left\{ \lambda_{\max} \left(\sum_{s=1}^N \mathbf{X}_s \right) \geq t \right\} \leq M e^{-t^2/8\sigma^2} \quad (44)$$

where $\sigma^2 = \left\| \sum_{s=1}^N \mathbf{A}_s^2 \right\|_2$.

C. Positive Definite Functions and Matrices

As part of our analysis, we need to show that a certain type of matrix is positive definite. To do this, we use a special class of functions that help define such matrices:

Definition 1 (Definition 6.15 from [73]): We will call a univariate function $\phi : [0, \infty) \rightarrow \mathbb{R}$ positive definite on \mathbb{R}^d if the corresponding multivariate function $\Psi(\mathbf{x}) = \phi(\|\mathbf{x}\|_2)$, $\mathbf{x} \in \mathbb{R}^d$, is positive definite. That is, for any finite sequence of distinct vectors $\{\mathbf{x}_r\}_{r=1}^n$ in \mathbb{R}^d , the matrix \mathbf{Z} defined as $Z_{rs} = \Psi(\mathbf{x}_r - \mathbf{x}_s)$ is positive definite.

The following theorem, which is a consequence of Schoenberg's theorem on the positive definiteness of completely monotone functions, provides the suitable tool for our purpose.

Theorem 4 (Theorem 7.15 from [73]): The inverse multi-quadratics $\phi(x) = (c^2 + x^2)^{-\beta}$ are positive definite functions on every \mathbb{R}^d , provided that $\beta > 0$ and $c > 0$.

APPENDIX II USEFUL LEMMAS

Lemma 3: Let $0 < \delta_m < \pi$, then the following equality holds:

$$\int_{-\pi+\delta_m}^{-\delta_m} \int_{\delta_m}^{\pi-\delta_m} \frac{1}{2 - 2\cos(\theta - \tau)} d\theta d\tau = -2 \ln \sin \delta_m. \quad (45)$$

Proof: The proof is a straightforward mathematical calculation. The LHS of (45) is simplified as follows:

$$\begin{aligned} &= \int_{-\pi+\delta_m}^{-\delta_m} \int_{\delta_m}^{\pi-\delta_m} \frac{1}{4 \sin^2(\frac{\theta-\tau}{2})} d\theta d\tau \\ &= \int_{-\pi+\delta_m}^{-\delta_m} \left(\frac{-1}{2} \cot\left(\frac{\theta-\tau}{2}\right) \right)_{\theta=\delta_m}^{\theta=\pi-\delta_m} d\tau \\ &= \int_{-\pi+\delta_m}^{-\delta_m} \frac{1}{2} \left(\cot\left(\frac{\delta_m-\tau}{2}\right) - \cot\left(\frac{\pi-\delta_m-\tau}{2}\right) \right) d\tau \\ &= \frac{1}{2} \left(\int_{-\pi+\delta_m}^{-\delta_m} \cot\left(\frac{\delta_m-\tau}{2}\right) d\tau - \int_{-\pi+\delta_m}^{-\delta_m} \tan\left(\frac{\delta_m+\tau}{2}\right) d\tau \right). \end{aligned}$$

We can calculate the integrals as follows:

$$\begin{aligned} &= \frac{1}{2} \left(\left(-2 \ln \sin\left(\frac{\delta_m-\tau}{2}\right) \right)_{-\pi+\delta_m}^{-\delta_m} \right. \\ &\quad \left. - \left(-2 \ln \cos\left(\frac{\tau+\delta_m}{2}\right) \right)_{-\pi+\delta_m}^{-\delta_m} \right) \\ &= \frac{1}{2} \left(-2 \ln \sin(\delta_m) + 2 \ln \sin\left(\frac{\pi}{2}\right) + \right. \\ &\quad \left. 2 \ln \cos(0) - 2 \ln \cos\left(\delta_m - \frac{\pi}{2}\right) \right) \\ &= \left(-\ln \sin(\delta_m) - \ln \cos\left(\delta_m - \frac{\pi}{2}\right) \right) \\ &= -2 \ln \sin(\delta_m). \end{aligned}$$

■

Lemma 4: Consider a stable LTI system with transfer function $G(z)$ and impulse response \mathbf{g} that satisfies Assumption 1. Let $\mathbf{z} \in \mathbb{C}^M$ satisfy Assumption 3, and let \mathbf{w} be the frequency response of G at these points. If M is sufficiently large, then the following bound holds:

$$\frac{\|L(\mathbf{w})\|_F}{\|\mathbf{w}\|_2} \leq 3 \sqrt{1 + \frac{2K}{\rho-1} \frac{\sqrt{-M \ln \sin \delta_m}}{\pi - 2\delta_m}}. \quad (46)$$

Proof: The Frobenius norm of the Loewner operator, scaled by the number of frequency points, is given by

$$\frac{\|L(\mathbf{w})\|_F^2}{M^2} = \frac{1}{M^2} \sum_{r=1}^M \sum_{s=1}^M \left| \frac{\bar{w}_r - w_s}{\bar{z}_r - z_s} \right|^2.$$

This summation can be approximated by a double integral of the function $f(\theta, \tau) = \left| \frac{G(e^{j\tau}) - G(e^{j\theta})}{e^{j\tau} - e^{j\theta}} \right|^2$, defined over the region $R = \{(\theta, \tau) \mid \theta \in [\delta_m, \pi - \delta_m], \tau \in [-\pi + \delta_m, -\delta_m]\}$. Since G is a rational function with no poles on the unit circle (recall that G is stable), it is smooth. Denote by C_r the upper bound on the absolute value of all of the r -th partial derivatives of f over the compact region R . Then, by the error bound for the midpoint composite rule in numerical integration (see Corollary 4.2 in [74]), we obtain:

$$\begin{aligned} &\frac{\|L(\mathbf{w})\|_F^2}{M^2} \\ &\leq \frac{1}{(\pi - 2\delta_m)^2} \int_{-\pi+\delta_m}^{-\delta_m} \int_{\delta_m}^{\pi-\delta_m} \left| \frac{G(e^{j\tau}) - G(e^{j\theta})}{e^{j\tau} - e^{j\theta}} \right|^2 d\theta d\tau \\ &\quad + \frac{C_1(\pi - 2\delta_m)}{2M} + \frac{C_2(\pi - 2\delta_m)^2}{4M^2}. \end{aligned} \quad (47)$$

We aim to find an upper bound for the integral in (47).

manipulate the integrand as follows

$$\begin{aligned}
& \left| \frac{G(e^{j\tau}) - G(e^{j\theta})}{e^{j\tau} - e^{j\theta}} \right|^2 = \frac{\left| \sum_{k=0}^{\infty} g_k e^{jk\tau} - \sum_{k=0}^{\infty} g_k e^{jk\theta} \right|^2}{2 - e^{j(\tau-\theta)} - e^{j(\theta-\tau)}} \\
& = \frac{\left| \sum_{k=0}^{\infty} g_k (e^{jk\tau} - e^{jk\theta}) \right|^2}{2 - 2 \cos(\theta - \tau)} \\
& = \frac{\left(\sum_{p=0}^{\infty} g_p (e^{-jp\tau} - e^{-jp\theta}) \right) \left(\sum_{q=0}^{\infty} g_q (e^{jq\tau} - e^{jq\theta}) \right)}{2 - 2 \cos(\theta - \tau)} \\
& = \frac{\sum_{p=0}^{\infty} \sum_{q=0}^{\infty} g_p g_q (e^{j\tau(q-p)} + e^{j\theta(q-p)})}{2 - 2 \cos(\theta - \tau)} \dots \\
& \quad - \frac{e^{j(q\tau-p\theta)} + e^{j(q\theta-p\tau)}}{2 - 2 \cos(\theta - \tau)}. \quad (48)
\end{aligned}$$

Each complex exponential term is bounded by 1, and thus, by the application of the triangle inequality, their summation is bounded by four. This results in the inequality

$$\left| \frac{G(e^{j\tau}) - G(e^{j\theta})}{e^{j\tau} - e^{j\theta}} \right|^2 \leq \frac{4 \left| \sum_{p=0}^{\infty} \sum_{q=0}^{\infty} g_p g_q \right|}{2 - 2 \cos(\theta - \tau)}.$$

Breaking the double summation into two parts, we obtain

$$\begin{aligned}
& \leq \frac{4 \left| \sum_{p=0}^{\infty} (g_p^2) + 2 \sum_{p=0}^{\infty} \sum_{s=1}^{\infty} (g_p g_{p+k}) \right|}{2 - 2 \cos(\theta - \tau)} \\
& \leq \frac{4 \left| \sum_{p=0}^{\infty} (g_p^2) + 2 \sum_{p=0}^{\infty} \sum_{k=1}^{\infty} (g_p^2 K \rho^{-k}) \right|}{2 - 2 \cos(\theta - \tau)} \\
& \leq \frac{4 \left(1 + \frac{2K}{\rho-1} \right) \sum_{p=0}^{\infty} (g_p^2)}{2 - 2 \cos(\theta - \tau)} = \frac{4 \left(1 + \frac{2K}{\rho-1} \right) \|\mathbf{g}\|_2^2}{2 - 2 \cos(\theta - \tau)}. \quad (49)
\end{aligned}$$

Because the integrand in (47) is upper bounded by (49), we find the following upper bound

$$\begin{aligned}
& \frac{\|L(\mathbf{w})\|_F^2}{M^2} \leq \\
& \frac{4 \left(1 + \frac{2K}{\rho-1} \right) \|\mathbf{g}\|_2^2}{(\pi - 2\delta_m)^2} \int_{-\pi+\delta_m}^{-\delta_m} \int_{\delta_m}^{\pi-\delta_m} \frac{1}{2 - 2 \cos(\theta - \tau)} d\theta d\tau \\
& + \frac{C_1(\pi - 2\delta_m)}{2M} + \frac{C_2(\pi - 2\delta_m)^2}{4M^2} \\
& = \frac{-8 \ln \sin \delta_m}{(\pi - 2\delta_m)^2} \left(1 + \frac{2K}{\rho-1} \right) \|\mathbf{g}\|_2^2 \\
& + \frac{C_1(\pi - 2\delta_m)}{2M} + \frac{C_2(\pi - 2\delta_m)^2}{4M^2} \quad (50)
\end{aligned}$$

in which we leveraged Lemma 3 to take the integral. On the other hand, by Parseval's theorem, we have

$$\|\mathbf{g}\|_2^2 = \frac{1}{2\pi} \int_{-\pi}^{\pi} |G(e^{j\theta})|^2 d\theta.$$

Applying the composite midpoint rule in numerical integration, we obtain

$$\left| \frac{1}{M} \|\mathbf{w}\|_2^2 - \|\mathbf{g}\|_2^2 \right| \leq \frac{4\pi^2 D_2}{24M^2},$$

where D_2 is an upper bound on the second derivative of $|G(e^{j\theta})|^2$ over the unit circle. Removing the absolute value,

we derive

$$\frac{1}{M} \|\mathbf{w}\|_2^2 \geq \|\mathbf{g}\|_2^2 - \frac{4\pi^2 D_2}{24M^2}. \quad (51)$$

Combining (50) and (51) results in

$$\begin{aligned}
& \frac{\|L(\mathbf{w})\|_F^2}{M \|\mathbf{w}\|_2^2} \leq \\
& \frac{\frac{-8 \ln \sin \delta_m}{(\pi - 2\delta_m)^2} \left(1 + \frac{2K}{\rho-1} \right) \|\mathbf{g}\|_2^2 + \frac{C_1(\pi - 2\delta_m)}{2M} + \frac{C_2(\pi - 2\delta_m)^2}{4M^2}}{\|\mathbf{g}\|_2^2 - \frac{4\pi^2 D_2}{24M^2}}. \quad (52)
\end{aligned}$$

Choose M large enough such that for some $0 < \epsilon < 1$ the following two conditions hold:

- The denominator in (52) is greater than or equal to $(1 - \epsilon) \|\mathbf{g}\|_2^2$.
- The numerator in (52) is less than or equal to $(1 + \epsilon) \frac{-8 \ln \sin \delta_m}{(\pi - 2\delta_m)^2} \left(1 + \frac{2K}{\rho-1} \right) \|\mathbf{g}\|_2^2$.

Consequently, we deduce

$$\frac{\|L(\mathbf{w})\|_F^2}{M \|\mathbf{w}\|_2^2} \leq \frac{-8 \ln \sin \delta_m}{(\pi - 2\delta_m)^2} \left(1 + \frac{2K}{\rho-1} \right) \frac{1 + \epsilon}{1 - \epsilon}. \quad (53)$$

This upper bound holds for any $0 < \epsilon < 1$. In particular, choosing $\epsilon = \frac{1}{17}$ establishes the bound stated in the theorem. ■

Lemma 5: Let L be the Laplacian of a weighted graph with n nodes and denote the weight between nodes r and s with w_{rs} . Assume $w_{rs} \geq c$ for some $c > 0$. Denote the r -th eigenvalue of L by $\lambda_r(L)$. The following bound holds:

$$\lambda_{n-1}(L) \geq cn. \quad (54)$$

Proof: From the Rayleigh quotient we have

$$\begin{aligned}
\lambda_{n-1}(L) & = \min_{\|x\|_2=1, x^\top \mathbf{1}_n=0} x^\top L x \\
& = \min_{\|x\|_2=1, x^\top \mathbf{1}_n=0} \sum_{r,s} w_{rs} (x_r - x_s)^2 \\
& \geq c \min_{\|x\|_2=1, x^\top \mathbf{1}_n=0} \sum_{r,s} (x_r - x_s)^2 = c \lambda_{n-1}(L_{comp})
\end{aligned}$$

in which L_{comp} is the Laplacian of a complete graph with n nodes. The proof is complete by the fact that $\lambda_{n-1}(L_{comp}) = n$. ■

Lemma 6: Let $\mathbf{z} \in \mathbb{C}^M$ satisfy Assumption 3. Then the matrix $\mathbf{X} \in \mathbb{C}^{M \times M}$ defined as $\mathbf{X}_{rs} = \frac{2}{|\bar{z}_r - z_s|^2}$ is positive definite.

Proof: First, note that by Assumption 3, there exists a frequency margin δ_m that ensures \mathbf{X} is well-defined, as the denominator of $\frac{2}{|\bar{z}_r - z_s|^2}$ is nonzero. By applying Theorem 4, the matrix $\mathbf{Y} \in \mathbb{C}^{M \times M}$, defined as

$$\mathbf{Y}_{rs} = \frac{2}{c^2 + |\bar{z}_r - z_s|^2},$$

is positive definite. On the other hand,

$$\begin{aligned} \|\mathbf{X} - \mathbf{Y}\|_2^2 &\leq \|\mathbf{X} - \mathbf{Y}\|_F^2 \\ &\leq \sum_{r,s=1}^M \left(\frac{2}{|\bar{z}_r - z_s|^2} - \frac{2}{c^2 + |\bar{z}_r - z_s|^2} \right)^2 \\ &= \sum_{r,s=1}^M \frac{4c^4}{|\bar{z}_r - z_s|^4 (|\bar{z}_r - z_s|^2 + c^2)^2} \\ &\leq \frac{4Mc^4}{\delta_m^4 (\delta_m^2 + c^2)^2}. \end{aligned}$$

Thus, the following bound holds:

$$\|\mathbf{X} - \mathbf{Y}\|_2 \leq \frac{2c^2\sqrt{M}}{\delta_m^2(\delta_m^2 + c^2)},$$

where the RHS tends to zero as c approaches zero. Therefore, since the eigenvalue as a function of the matrix is continuous, by choosing $c > 0$ sufficiently small, we can make the eigenvalues of \mathbf{X} arbitrarily close to those of \mathbf{Y} , which completes the proof. ■

Lemma 7: Let $\mathbf{z} \in \mathbb{C}^M$ satisfy Assumption 3. Then,

$$\frac{1}{M^2} \sum_{r=1}^M \sum_{s=1}^M \frac{1}{|\bar{z}_r - z_s|^2} \leq \frac{-2 \ln \sin(\delta_m)}{(\pi - 2\delta_m)^2}. \quad (55)$$

Proof: Similar to (48), the summation on the LHS simplifies to

$$\frac{1}{M^2} \sum_{r=1}^M \sum_{s=1}^M \frac{1}{2 - 2\cos(\theta_s - \tau_r)},$$

where $\tau_r = -\theta_r$. The function $\frac{1}{2 - 2\cos(\theta - \tau)}$ over $\theta \in [0, \pi]$ and $\tau \in [-\pi, 0]$ is convex; Thus, the composite midpoint rule underestimates the integral. Therefore,

$$\begin{aligned} \frac{1}{M^2} \sum_{r=1}^M \sum_{s=1}^M \frac{1}{|\bar{z}_r - z_s|^2} &\leq \\ &\frac{1}{(\pi - 2\delta_m)^2} \int_{-\pi+\delta_m}^{-\delta_m} \int_{\delta_m}^{\pi-\delta_m} \frac{1}{2 - 2\cos(\theta - \tau)} d\theta d\tau. \end{aligned}$$

The proof is complete by applying Lemma 3 to evaluate the integral. ■

ACKNOWLEDGMENT

The authors thank Reza Vafaei for helpful discussions.

REFERENCES

- [1] K. J. Keesman, *System identification: an introduction*. Springer Science & Business Media, 2011.
- [2] D. Tse, M. Dahleh, and J. Tsitsiklis, "Optimal asymptotic identification under bounded disturbances," *IEEE Transactions on Automatic Control*, vol. 38, no. 8, pp. 1176–1190, 1993.
- [3] S. Ko, E. Weyer, and M. C. Campi, "Non-asymptotic model quality assessment of transfer functions at multiple frequency points," *Automatica*, vol. 60, pp. 65–78, 2015.
- [4] Y. Li, J. Yu, L. Conger, T. Kargin, and A. Wierman, "Learning the uncertainty sets of linear control systems via set membership: A non-asymptotic analysis," in *Forty-first International Conference on Machine Learning*, 2024.
- [5] E. Sahinoglu and S. Shahrapour, "An online optimization perspective on first-order and zero-order decentralized nonsmooth nonconvex stochastic optimization," in *Proceedings of the 41st International Conference on Machine Learning*, 2024, pp. 43 043–43 059.
- [6] S. Sun and Y. Mo, "Non-asymptotic analysis of subspace identification for stochastic systems using multiple trajectories," *arXiv preprint arXiv:2501.18853*, 2025.
- [7] Y. Sattar, Y. Jedra, M. Fazel, and S. Dean, "Finite sample identification of partially observed bilinear dynamical systems," *arXiv preprint arXiv:2501.07652*, 2025.
- [8] A. Honarpisheh, M. Bozdag, O. Camps, and M. Sznaier, "Generalization error analysis for selective state-space models through the lens of attention," 2025. [Online]. Available: <https://arxiv.org/abs/2502.01473>
- [9] C. De Persis and P. Tesi, "Formulas for data-driven control: Stabilization, optimality, and robustness," *IEEE Transactions on Automatic Control*, vol. 65, no. 3, pp. 909–924, 2019.
- [10] J. Coulson, J. Lygeros, and F. Dörfler, "Data-enabled predictive control: In the shallows of the deepc," in *2019 18th European control conference (ECC)*. IEEE, 2019, pp. 307–312.
- [11] A. Oliveira, J. Zheng, and M. Sznaier, "Convex data-driven contraction with riemannian metrics," *IEEE Control Systems Letters*, 2025.
- [12] H. Yin, P. Seiler, and M. Arcak, "Stability analysis using quadratic constraints for systems with neural network controllers," *IEEE Transactions on Automatic Control*, vol. 67, no. 4, pp. 1980–1987, 2021.
- [13] H. M. Hedesh and M. Siami, "Ensuring both positivity and stability using sector-bounded nonlinearity for systems with neural network controllers," *IEEE Control Systems Letters*, vol. 8, pp. 1685–1690, 2024.
- [14] H. M. Hedesh, M. K. Wafi, and M. Siami, "Local stability and region of attraction analysis for neural network feedback systems under positivity constraints," *arXiv preprint arXiv:2505.22889*, 2025.
- [15] R. Vafaei and M. Siami, "Learning-based sparse sensing with performance guarantees," *IEEE Transactions on Automatic Control*, vol. 70, no. 1, pp. 387–402, 2024.
- [16] B. Recht, "A tour of reinforcement learning: The view from continuous control," *Annual Review of Control, Robotics, and Autonomous Systems*, vol. 2, no. 1, pp. 253–279, 2019.
- [17] M. Simchowitz, H. Mania, S. Tu, M. I. Jordan, and B. Recht, "Learning without mixing: Towards a sharp analysis of linear system identification," in *Conference On Learning Theory*. PMLR, 2018, pp. 439–473.
- [18] A. Chiuso and G. Pilonetto, "System identification: A machine learning perspective," *Annual Review of Control, Robotics, and Autonomous Systems*, vol. 2, no. 1, pp. 281–304, 2019.
- [19] S. Tu, R. Frostig, and M. Soltanolkotabi, "Learning from many trajectories," *Journal of Machine Learning Research*, vol. 25, no. 216, pp. 1–109, 2024.
- [20] R. Pintelon and J. Schoukens, *System identification: a frequency domain approach*. John Wiley & Sons, 2012.
- [21] T. McKelvey, "Frequency domain identification methods," *Circuits, Systems and Signal Processing*, vol. 21, no. 1, pp. 39–55, 2002.
- [22] P. A. Parrilo, M. Sznaier, R. S. Pena, and T. Inanc, "Mixed time/frequency-domain based robust identification," *Automatica*, vol. 34, no. 11, pp. 1375–1389, 1998.
- [23] A. Devonport, P. Seiler, and M. Arcak, "Frequency domain gaussian process models for h_∞ uncertainties," in *Proceedings of The 5th Annual Learning for Dynamics and Control Conference*, ser. Proceedings of Machine Learning Research, N. Matni, M. Morari, and G. J. Pappas, Eds., vol. 211. PMLR, 15–16 Jun 2023, pp. 1046–1057. [Online]. Available: <https://proceedings.mlr.press/v211/devonport23a.html>
- [24] M. Abdalmoaty, J. Miller, M. Yin, and R. S. Smith, "Frequency-domain identification of discrete-time systems using sum-of-rational optimization," *IFAC-PapersOnLine*, vol. 58, no. 15, pp. 121–126, 2024.
- [25] M. Fazel, T. K. Pong, D. Sun, and P. Tseng, "Hankel matrix rank minimization with applications to system identification and realization," *SIAM Journal on Matrix Analysis and Applications*, vol. 34, no. 3, pp. 946–977, 2013.
- [26] G. Pilonetto, T. Chen, A. Chiuso, G. De Nicolao, and L. Ljung, "Regularized linear system identification using atomic, nuclear and kernel-based norms: The role of the stability constraint," *Automatica*, vol. 69, pp. 137–149, 2016.
- [27] M. Khosravi, M. Yin, A. Iannelli, A. Parsi, and R. S. Smith, "Low-complexity identification by sparse hyperparameter estimation," *IFAC-PapersOnLine*, vol. 53, no. 2, pp. 412–417, 2020.
- [28] B. Yilmaz, K. Bekiroglu, C. Lagoa, and M. Sznaier, "A randomized algorithm for parsimonious model identification," *IEEE Transactions on Automatic Control*, vol. 63, no. 2, pp. 532–539, 2017.

- [29] R. S. Smith, "Frequency domain subspace identification using nuclear norm minimization and hankel matrix realizations," *IEEE Transactions on Automatic Control*, vol. 59, no. 11, pp. 2886–2896, 2014.
- [30] M. Sznaier, M. Ayazoglu, and T. Inanc, "Fast structured nuclear norm minimization with applications to set membership systems identification," *IEEE Transactions on Automatic Control*, vol. 59, no. 10, pp. 2837–2842, 2014.
- [31] A. Tsiamis, I. Ziemann, N. Matni, and G. J. Pappas, "Statistical learning theory for control: A finite-sample perspective," *IEEE Control Systems Magazine*, vol. 43, no. 6, pp. 67–97, 2023.
- [32] M. Bozdag, A. Honarpisheh, and M. Sznaier, "Safe control for pursuit-evasion with density functions," *IEEE Control Systems Letters*, 2025.
- [33] Y. Jedra and A. Proutiere, "Sample complexity lower bounds for linear system identification," in *2019 IEEE 58th Conference on Decision and Control (CDC)*, 2019, pp. 2676–2681.
- [34] T. Sarkar and A. Rakhlin, "Near optimal finite time identification of arbitrary linear dynamical systems," in *International Conference on Machine Learning*. PMLR, 2019, pp. 5610–5618.
- [35] A. Tsiamis and G. J. Pappas, "Finite sample analysis of stochastic system identification," in *2019 IEEE 58th Conference on Decision and Control (CDC)*, 2019, pp. 3648–3654.
- [36] Y. Zheng and N. Li, "Non-asymptotic identification of linear dynamical systems using multiple trajectories," *IEEE Control Systems Letters*, vol. 5, no. 5, pp. 1693–1698, 2020.
- [37] S. Oymak and N. Ozay, "Revisiting ho–kalman-based system identification: Robustness and finite-sample analysis," *IEEE Transactions on Automatic Control*, vol. 67, no. 4, pp. 1914–1928, 2021.
- [38] S. Fattahi and S. Sojoudi, "Sample complexity of block-sparse system identification problem," *IEEE Transactions on Control of Network Systems*, vol. 8, no. 4, pp. 1905–1917, 2021.
- [39] I. M. Ziemann, H. Sandberg, and N. Matni, "Single trajectory nonparametric learning of nonlinear dynamics," in *Proceedings of Thirty Fifth Conference on Learning Theory*, ser. Proceedings of Machine Learning Research, P.-L. Loh and M. Raginsky, Eds., vol. 178. PMLR, 02–05 Jul 2022, pp. 3333–3364. [Online]. Available: <https://proceedings.mlr.press/v178/ziemann22a.html>
- [40] N. Chatzikiriakos and A. Iannelli, "Sample complexity bounds for linear system identification from a finite set," *IEEE Control Systems Letters*, vol. 8, pp. 2751–2756, 2024.
- [41] P. Shah, B. N. Bhaskar, G. Tang, and B. Recht, "Linear system identification via atomic norm regularization," in *2012 IEEE 51st IEEE conference on decision and control (CDC)*. IEEE, 2012, pp. 6265–6270.
- [42] T. Sarkar, A. Rakhlin, and M. A. Dahleh, "Finite time lti system identification," *Journal of Machine Learning Research*, vol. 22, no. 26, pp. 1–61, 2021. [Online]. Available: <http://jmlr.org/papers/v22/19-725.html>
- [43] A. Tsiamis, M. Abdalmoaty, R. S. Smith, and J. Lygeros, "Finite sample frequency domain identification," in *2024 IEEE 63rd Conference on Decision and Control (CDC)*, 2024, pp. 3025–3030.
- [44] L. Ljung, "System identification," in *Signal analysis and prediction*. Springer, 1998, pp. 163–173.
- [45] D. Karachalios, I. V. Gosea, and A. C. Antoulas, "The loewner framework for system identification and reduction," in *Model Order Reduction: Volume I: System-and Data-Driven Methods and Algorithms*. de Gruyter, 2021, pp. 181–228.
- [46] J. Simard, "Interpolation and model reduction of nonlinear systems in the loewner framework," Ph.D. dissertation, Imperial College London, 2023.
- [47] A. Moreschini, J. D. Simard, and A. Astolfi, "Data-driven model reduction for port-hamiltonian and network systems in the loewner framework," *Automatica*, vol. 169, p. 111836, 2024.
- [48] M. Scandella, A. Moreschini, and T. Parisini, "Kernel-based continuous-time system identification: A parametric approximation," in *2023 62nd IEEE Conference on Decision and Control (CDC)*. IEEE, 2023, pp. 1492–1497.
- [49] R. Singh and M. Sznaier, "A loewner matrix based convex optimization approach to finding low rank mixed time/frequency domain interpolants," in *2020 American Control Conference (ACC)*. IEEE, 2020, pp. 5169–5174.
- [50] A. Honarpisheh, R. Singh, J. Miller, and M. Sznaier, "Identification of low order systems in a loewner framework," *IFAC-PapersOnLine*, vol. 58, no. 15, pp. 199–204, 2024.
- [51] A. Mayo and A. Antoulas, "A framework for the solution of the generalized realization problem," *Linear Algebra and its Applications*, vol. 425, no. 2, pp. 634–662, 2007, special Issue in honor of Paul Fuhrmann.
- [52] M. Fazel, H. Hindi, and S. P. Boyd, "A rank minimization heuristic with application to minimum order system approximation," in *Proceedings of the 2001 American control conference.(Cat. No. O1CH37148)*, vol. 6. IEEE, 2001, pp. 4734–4739.
- [53] T. McKelvey, "Frequency domain identification," *IFAC Proceedings Volumes*, vol. 33, no. 15, pp. 7–18, 2000.
- [54] J. Schoukens, R. Pintelon, and Y. Rolain, "Time domain identification, frequency domain identification. equivalencies! differences?" in *Proceedings of the 2004 American Control Conference*, vol. 1. IEEE, 2004, pp. 661–666.
- [55] A. C. Antoulas, S. Lefteriu, A. C. Ionita, P. Benner, and A. Cohen, "A tutorial introduction to the loewner framework for model reduction," *Model Reduction and Approximation: Theory and Algorithms*, vol. 15, p. 335, 2017.
- [56] I. Ziemann, A. Tsiamis, B. Lee, Y. Jedra, N. Matni, and G. J. Pappas, "A tutorial on the non-asymptotic theory of system identification," in *2023 62nd IEEE Conference on Decision and Control (CDC)*, 2023, pp. 8921–8939.
- [57] N. Parikh, S. Boyd *et al.*, "Proximal algorithms," *Foundations and trends® in Optimization*, vol. 1, no. 3, pp. 127–239, 2014.
- [58] T. Hoheisel and E. Paquette, "Uniqueness in nuclear norm minimization: Flatness of the nuclear norm sphere and simultaneous polarization," *Journal of Optimization Theory and Applications*, vol. 197, no. 1, pp. 252–276, 2023.
- [59] B. N. Bhaskar, G. Tang, and B. Recht, "Atomic norm denoising with applications to line spectral estimation," *IEEE Transactions on Signal Processing*, vol. 61, no. 23, pp. 5987–5999, 2013.
- [60] T. Hastie, R. Tibshirani, J. H. Friedman, and J. H. Friedman, *The elements of statistical learning: data mining, inference, and prediction*. Springer, 2009, vol. 2.
- [61] B. Recht, M. Fazel, and P. A. Parrilo, "Guaranteed minimum-rank solutions of linear matrix equations via nuclear norm minimization," *SIAM review*, vol. 52, no. 3, pp. 471–501, 2010.
- [62] E. Candes and B. Recht, "Exact matrix completion via convex optimization," *Communications of the ACM*, vol. 55, no. 6, pp. 111–119, 2012.
- [63] J.-F. Cai, X. Qu, W. Xu, and G.-B. Ye, "Robust recovery of complex exponential signals from random gaussian projections via low rank hankel matrix reconstruction," *Applied and Computational Harmonic Analysis*, vol. 41, no. 2, pp. 470–490, 2016. [Online]. Available: <https://www.sciencedirect.com/science/article/pii/S1063520316000117>
- [64] Y. Sun, S. Oymak, and M. Fazel, "Finite sample identification of low-order lti systems via nuclear norm regularization," *IEEE Open Journal of Control Systems*, vol. 1, pp. 237–254, 2022.
- [65] G. A. Watson, "Characterization of the subdifferential of some matrix norms," *Linear Algebra Appl.*, vol. 170, no. 1, pp. 33–45, 1992.
- [66] Z. Drmač and B. Peherstorfer, "Learning low-dimensional dynamical-system models from noisy frequency-response data with loewner rational interpolation," in *Realization and Model Reduction of Dynamical Systems: A Festschrift in Honor of the 70th Birthday of Thanos Antoulas*. Springer, 2022, pp. 39–57.
- [67] J. Chen, C. Nett, and M. Fan, "Worst case system identification in h_{∞} : validation of a priori information, essentially optimal algorithms, and error bounds," *IEEE Transactions on Automatic Control*, vol. 40, no. 7, pp. 1260–1265, 1995.
- [68] A. Mashhadireza, N. D. Dehnavi, A. Sadighi, and M. Bitaraf, "Detection of anomalous behavior of a scaled laboratory structure based on stochastic subspace identification method," in *2022 10th RSI International Conference on Robotics and Mechatronics (ICRoM)*. IEEE, Nov. 2022.
- [69] A. Mashhadireza, A. Sadighi, M. Bitaraf, and N. Dehghani Dehnavi, "Novelty detection in laboratory structure using stochastic subspace identification and a novel non-destructive experimental method for damping changes," *Struct. Eng. Int.*, vol. 35, no. 4, pp. 604–616, Oct. 2025.
- [70] H. H. Bauschke and P. L. Combettes, *Convex Analysis and Monotone Operator Theory in Hilbert Spaces*. Springer, 2017.
- [71] M. Vidyasagar and R. L. Karandikar, "A learning theory approach to system identification and stochastic adaptive control," *Probabilistic and randomized methods for design under uncertainty*, pp. 265–302, 2006.
- [72] J. A. Tropp, "User-friendly tail bounds for sums of random matrices," *Foundations of computational mathematics*, vol. 12, pp. 389–434, 2012.
- [73] H. Wendland, *Scattered data approximation*. Cambridge university press, 2004, vol. 17.
- [74] C. J. Grant and E. Talvila, "Elementary numerical methods for double integrals," *Minnesota Journal of Undergraduate Mathematics*, vol. 4, no. 1, May 2021. [Online]. Available: <https://pubs.lib.umn.edu/index.php/mjum/article/view/4157>



Arya Honarpisheh (Graduate Student Member, IEEE) is a Ph.D. student in Electrical Engineering at Northeastern University, Boston, MA, USA. He is a graduate research assistant in the Robust Systems Lab under the supervision of Mario Sznaier. Prior to his Ph.D., he earned a Bachelor of Science in Mechanical Engineering from Sharif University of Technology, Tehran, Iran. His research interests include system identification, statistical learning, and control theory.



Mario Sznaier (Fellow, IEEE) is currently the Dennis Picard Chaired Professor at the Electrical and Computer Engineering Department, Northeastern University, Boston. Prior to joining Northeastern University, Dr. Sznaier was a Professor of Electrical Engineering at the Pennsylvania State University and also held visiting positions at the California Institute of Technology. His research interest include robust identification and control of hybrid systems, robust optimization, and learning enabled control. Dr.

Sznaier is currently serving as Editor in Chief of the section on AI and Control of the journal *Frontiers in Control Engineering*, and vice-chair of IFAC's Coordinating Committee CC 2, Design Methods. Additional service includes Associate Editor for the *Journal Automatica* (2005-2021), General co-Chair of the 2016 MSC, and Program Chair of the 2017 CDC. He is a distinguished member of the IEEE Control Systems Society and is a Fellow of IEEE and IFAC.